

LTR-CDME-05-32-NP, Rev. 2

**Limited Inspection of the Steam Generator
Tube Portion Within the Tubesheet
at Byron 2 & Braidwood 2**

August 2005

Author: /s/ Gary W. Whiteman

Gary W. Whiteman

Regulatory Compliance and Plant Licensing

Verified: /s/ Robert F. Keating

Robert F. Keating

Major Component Replacements & Engineering

Westinghouse Electric Company LLC

P.O. Box 355

Pittsburgh, PA 15230-0355

© 2005 Westinghouse Electric Company LLC

All Rights Reserved

Official Record Electronically Approved in EDMS

This page intentionally blank.

Revision Log

Revision	Changes
0	(original issue)
1	<p>General:</p> <ul style="list-style-type: none"> - Minor typographical corrections - Added new reference as Reference 9; other references indexed accordingly <p>Section 1, Introduction</p> <ul style="list-style-type: none"> - Added "diameter and thickness" in 2nd paragraph. - Changed 4.23 to 4.26 and 21.23 to 21.26 in 4th paragraph. - Added "including some extending into the tube" in 3) - Deleted "exigent"; revised last sentence in 6th paragraph. - Replaced "remaining in" with "below" in last sentence, 7th paragraph. <p>Section, 3 Historical Background...</p> <ul style="list-style-type: none"> - Changed Reference 15 to 17 in 2nd paragraph. <p>Section 5, Structural Analysis...</p> <ul style="list-style-type: none"> - Added reference 14 in 2nd paragraph. <p>Section 6.0, Leak Rate Analysis...</p> <ul style="list-style-type: none"> - Added "and the fall 2005 outage for Byron 2" after Braidwood 2.
2	<p>General</p> <ul style="list-style-type: none"> - The report has been revised in support of obtaining permanent Technical Specification (TS) changes for the limited SG tube joint inspection with the rotating probe coil (RPC) - Three sections were added and the remainder were indexed accordingly <ul style="list-style-type: none"> • A new section on plant operating conditions was added (Section 5.0) • A new section of steam generator tube pull test program was added (Section 6.0) • A new section to further substantiate qualitative arguments used by NRC Staff for one cycle approval of the limited RPC inspection was added (Section 9.0) <ul style="list-style-type: none"> - Figures and tables were placed at the end of sections in which they are referenced and renumbered accordingly - Appendix A, Structural Analysis, was incorporated into the document as a revised section (Section 7.0)

	<ul style="list-style-type: none"> - List of references from former Appendix A was combined with previous list of references and the list of references has been renumbered accordingly. - List of tables and figures has been revised to reflect the addition of new sections in the report; new figures were added to demonstrate steam generator tube pull out test results; new tables were added to address the effects of tube hole dilation in the tubesheet during all plant conditions and contact pressure for experimental loss coefficients - The table of contents was revised accordingly <p>Section 1, Introduction</p> <ul style="list-style-type: none"> - Text was revised to incorporate H* methodology into the letter report - Text referencing Appendix A was removed - An overview of the sections in the report was revised to reflect the new listing of sections. <p>Section 2, Summary Discussion</p> <ul style="list-style-type: none"> - Text referencing alternate leak rate prediction analyses were removed. <p>Section 8, Leak Rate Analysis of Cracked Tube-to-Tubesheet Joints</p> <ul style="list-style-type: none"> - The alternate SLB leak rate calculation was removed from text - One cycle approval discussion removed for Byron 2, Braidwood 2 - Additional information of Darcy expression for flow rate through a porous media was added - Ligament tearing discussion (Section 8.2) was added to text. <p>Section 12, Recommended Inspection Plans</p> <ul style="list-style-type: none"> - Discussion on one cycle approval or TJ RPC inspection length was removed. <p>Section 13, References</p> <ul style="list-style-type: none"> - Unused references from previous reference list were removed.
--	---

Abstract

Nondestructive examination indications of primary water stress corrosion cracking were found in the Alloy 600 thermally treated Westinghouse Model D5 steam generator tubes at the Catawba 2 nuclear power plant in the fall of 2004. Most of the indications were located in the tube-to-tubesheet welds with a few of the indications being reported as extending into the parent tube. In addition, a small number of tubes were reported with indications about 3/4 inch above the bottom of the tube, and multiple indications were reported in one tube at internal bulge locations in the upper third of the tubesheet. The tube end weld indications were dominantly axial in orientation and almost all of the indications were concentrated in one steam generator. Circumferential cracks were also reported at internal bulge locations in two of the Alloy 600 thermally treated steam generator tubes at the Vogtle 1 plant site in the spring of 2005. Based on interpretations of requirements published by the NRC staff in GL 2004-01, Exelon requested that a recommendation be developed for examination of the Westinghouse Model D5 steam generator tubesheet regions at the Byron 2 and Braidwood 2 power plants. An evaluation was performed that considered the requirements of the ASME Code, Regulatory Guides, NRC Generic Letters, NRC Information Notices, the Code of Federal Regulations, NEI 97-06, and additional industry requirements. The conclusion of the technical evaluation is that the structural integrity of the primary-to-secondary pressure boundary is unaffected by degradation of any level below a depth of 17 inches from the top of the 21 inch thick tubesheet or the tube end welds because the tube-to-tubesheet hydraulic joints make it extremely unlikely that any operating or faulted condition loads are applied to the tube tack expanded region or the tube welds. Internal tube bulges, i.e., within the tubesheet, were created in a number of tubes as an artifact of the manufacturing process. The possibility of degradation at these locations exists based on the reported degradation at Catawba 2 and Vogtle 1. A recommendation is made for examination of a sample of the tubes to a depth of 17 inches below the top of the tubesheet based on the use of a bounding leak rate evaluation and the application of a structural analysis of this report. Application of the bounding leak rate and structural analysis approaches supporting this conclusion requires the approval of the NRC staff through a license amendment because it is based on a redefinition of the primary-to-secondary pressure boundary relative to the original design of the plant.

This page intentionally blank.

Table of Contents

Revision Log.....	3
Abstract	5
1.0 Introduction	11
2.0 Summary Discussion	17
3.0 Historical Background Regarding Tube Indications in the Tubesheet	21
4.0 Design Requirements for the Tube-to-Tubesheet Joint Region.....	23
5.0 Operating Conditions.....	25
5.1 Normal Operating Conditions	25
5.2 Faulted Conditions	25
6.0 Steam Generator Tube Leakage and Pullout Test Program Discussion.....	27
6.1 Model F Tube Joint Leakage Resistance Program.....	27
6.1.1 Test Sample Configuration	28
6.2 Model D5 Tube Joint Leakage Resistance Program	30
6.2.1 Test Sample Configuration	32
6.3 Model D5 Tube Joint Pullout Resistance Program	33
6.4 Test Procedure	33
6.4.1 Model F Leakage Resistance Test.....	33
6.4.2 Model D5 Leakage Tests.....	34
6.4.3 Model D5 Mechanical Loading Tests.....	35
6.5 Test Summary	36
6.5.1 Leak Test Results	36
6.5.2 Model D5 Tube Pullout Test Results	36
7.0 Structural Analysis of Tube-to-Tubesheet Joint.....	45
7.1 Evaluation of Tubesheet Deflection Effects for Tube-to-Tubesheet Contact Pressure. 46	
7.1.1 Material Properties and Tubesheet Equivalent Properties	46
7.1.2 Finite Element Model	49
7.1.3 Tubesheet Rotation Effects.....	50
7.1.4 Byron/Braidwood 2 Contact Pressures	53
7.2 Determination of Required Engagement Length of the Tube in the Tubesheet	55

8.0	Leak Rate Analysis of Cracked Tube-to-Tubesheet Joints.....	74
8.1	The Bellwether Principle for Normal Operation to Steam Line Break Leak Rates	74
8.2	Ligament Tearing Discussion.....	78
9.0	Review of Qualitative Arguments Used by the NRC Staff for One Cycle Approval of the Tube Joint Eddy Current Inspection Length for Braidwood Unit 2	83
9.1	Joint Structural Integrity Discussion	83
9.1.1	Discussion of Interference Loads	84
9.1.2	Flexibility Discussion.....	86
9.1.3	Analysis.....	88
9.1.4	Conclusions.....	90
9.2	Joint Leakage Integrity Discussion.....	90
9.2.1	Loss Coefficient Contact Pressure Correlation.....	91
10.0	Conclusions and Inspection Recommendations	103
11.0	References.....	105

List of Tables

Table 6-1 Model F Leak Test Program Matrix.....	28
Table 6-2. Model D5 Leak Test Program Matrix.....	31
Table 7-1. Summary of Material Properties Alloy 600 Tube Material.....	59
Table 7-2. Summary of Material Properties for SA-508 Class 2a Tubesheet Material.....	59
Table 7-3. Summary of Material Properties SA-533 Grade A Class 2 Shell Material.....	59
Table 7-4. Summary of Material Properties SA-216 Grade WCC Channelhead Material.....	60
Table 7-5. Equivalent Solid Plate Elasticity Coefficients for D5 Perforated TS SA-508 Class 2a Tubesheet Material.....	60
Table 7-6. Tube/Tubesheet Maximum & Minimum Contact Pressures & H* for Byron/Braidwood Unit 2 Steam Generators.....	61
Table 7-7. Cumulative Forces Resisting Pull Out from the Top of the Tubesheet Byron/Braidwood 2 – Hot Leg Normal Conditions Low T_{ave} , High T_{sec}	62
Table 7-8. Cumulative Forces Resisting Pull Out from the TTS Byron/Braidwood 2 – Hot Leg Normal Conditions High T_{ave} , Low T_{sec}	63
Table 7-9. Cumulative Forces Resisting Pull Out from the TTS Byron/Braidwood 2–Faulted (SLB) Conditions.....	64
Table 7-10. Cumulative Forces Resisting Pull Out from the TTS Byron/Braidwood 2–FLB Conditions Low T_{ave} , High T_{sec}	65
Table 7-11. Cumulative Forces Resisting Pull Out for FLB Conditions High T_{ave} , Low T_{sec}	66
Table 7-12. Large Displacement, 0.25 in. Pullout Test Data.....	67
Table 7-13. Summary of H* Calculations for Byron/Braidwood Unit 2.....	67
Table 7-14. H* Summary Table.....	68
Table 9-1. Radial Flexibilities Times Elastic Modulus (in./psi).....	95
Table 9-2. Contact Pressure Influence Factors for Model F SG Tubes at 600°F.....	95
Table 9-2. Contact Pressure Influence Factors for Model F SG Tubes at 600°F.....	96
Table 9-3. Tubesheet Hole Diametral Dilatation for R18C77.....	97
Table 9-4. Contact Pressure for Experimental Loss Coefficients at Room Temperature Conditions.....	98
Table 9-5. Contact Pressure for Experimental Loss Coefficients at 600°F Heated Conditions.....	99

List of Figures

Figure 1-1. Distribution of Indications in SG A at Catawba 2.....	15
Figure 1-2. Distribution of Indications in SG B at Catawba 2.....	15
Figure 1-3. Distribution of Indications in SG D at Catawba 2	16
Figure 2-1. As-Fabricated & Analyzed Tube-to-Tubesheet Welds.....	20
Figure 6-1. Model F Leakage Test Schematic.....	38
Figure 6-2. Model F Tube Hydraulic Expansion Process Schematic	39
Figure 6-3. Model D5 Tube Joint Sample Leakage Test Configuration	40
Figure 6-4. Schematic for the Test Autoclave Systems for Leak Rate Testing	41
Figure 6-5. Model D5 Tube Joint Sample Pullout Test Configuration	42
Figure 6-6. Flow Resistance Curve	43
Figure 6-7. Model D5 Pullout Test Data from Several Samples	44
Figure 7-1. Definition of H* Zones.....	69
Figure 7-2. Finite Element Model of Model D5-3 Tubesheet Region.....	70
Figure 7-3. Contact Pressures for Normal Condition (T_{min}) at Byron/Braidwood 2.....	71
Figure 7-4. Contact Pressures for Normal Condition (T_{max}) at Byron and Braidwood Unit 2	71
Figure 7-6. Contact Pressures for FLB Faulted Condition at Byron and Braidwood 2 (T_{min})	72
Figure 7-7. Contact Pressures for FLB Faulted Condition at Byron and Braidwood 2 (T_{max})....	73
Figure 7-8. D5 Pullout Test Results for Force/inch at 0.25 inch Displacement.....	73
Figure 8-1. Change in contact pressure at 10.5 inches below the TTS	80
Figure 8-2. Change in contact pressure at 12.6 inches below the TTS	80
Figure 8-3. Change in contact pressure at 16.9 inches below the TTS	81
Figure 8-4. Change in contact pressure at the bottom of the tubesheet	81
Figure 8-5. Change in contact pressure at 8.25 inches below the TTS	82
Figure 9-1. Geometry of the Tube-to-Tubesheet Interface	100
Figure 9-2. Model for Initial Contact Pressure	100
Figure 9-3. Determination of Contact Pressure, Normal or Accident Operation	101
Figure 9-4. Loss Coefficient versus Contact Pressure for Model D5 and Model F Steam Generators	102

Limited Steam Generator Tube-in-Tubesheet Inspection at Byron 2 & Braidwood 2

1.0 Introduction

Indications of cracking were reported based on the results from the nondestructive, eddy current examination of the steam generator (SG) tubes during the fall 2004 outage at the Catawba 2 nuclear power plant operated by the Duke Power Company, References 1, 2, and 3. The tube indications at Catawba were reported about 7.6 inches from the top of the tubesheet in one tube, and just above the tube-to-tubesheet welds in a region of the tube known as the tack expansion (TE) in several other tubes. Finally, indications were also reported in the tube-end welds (TEWs), also known as tube-to-tubesheet welds, joining the tube to the tubesheet. The spatial distribution by row and column number is shown on Figure 1-1 for SG A, Figure 1-2 for SG B, and Figure 1-3 for SG D at Catawba. There were no indications in SG C. The Catawba 2 plant has Westinghouse designed, Model D5 SGs similar to those in service at the Exelon Corporation's Byron Unit 2 and Braidwood Unit 2 plant sites. Model D5 SGs were fabricated with Alloy 600TT (thermally treated) tubes. The other remaining plant with Westinghouse Model D5 steam generators, which belongs to another utility, has inspected 3% of the tubes in the hot leg of all steam generators from 3 inches above to 21 inches below the top of the tubesheet during 2R08 and has reported no indications. Regardless, there is a potential for tube indications similar to those reported at Catawba within the tubesheet region to be reported in the Braidwood 2 and Byron 2 SGs during future inspections. (Note: No indications were found during the planned inspection of the Braidwood 2 SG tubes in April 2005 as described herein. Moreover, no indications were found during a somewhat similar inspection of the tubes in two SGs at Wolf Creek in April 2005.)

It was subsequently noted that an indication was reported in each of two SG tubes at the Vogtle Unit 1 plant operated by the Southern Nuclear Operating Company (Reference 4). The Vogtle SGs are of the Westinghouse Model F design with slightly smaller, diameter and thickness, A600TT tubes.

The SGs for all four Model D5 plant sites were fabricated in the 1978 to 1980 timeframe using similar manufacturing processes with a few exceptions. For example, the fabrication technique used for the installation of the SG tubes at Braidwood 2 would be expected to lead to a much lower likelihood for crack-like indications to be present in the region known as the tack expansion relative to Catawba 2 because a different process for effecting the tack expansions was adopted prior to the time of the fabrication of the Braidwood 2 SGs. The same statement cannot be made with regard to the tack expansion region in the Byron 2 SGs since they were fabricated at about the same time as the Catawba 2 SGs using the same tack expansion process.

A recommended examination plan, consistent with Reference 6, for the tubes and welds is delineated in Section 12.0 of this report. With regard to the tack expansion region of the tube and

the tube end welds, the recommendation is to not perform any specific inspection of the SG tubes at either the Byron 2 or Braidwood 2 plant sites. The H* methodology is valid for use in supporting the application of a recently developed independent leakage evaluation methodology based on the change in contact pressure between the tube and the tubesheet between normal operation and postulated accident conditions. Moreover, in order to address potential uncertainties associated with the determination of specific leak rates, Exelon decided to set the depth of RPC inspection of the tubes to 17 inches from the top of tubesheet (TTS). This allows the use of the newly developed leak rate methodologies since excluded potential degradation regions would be limited to the bottom 4.26 inches of the tube in the nominally 21.26 inch thick tubesheet, which is well below the mid-plane of the tubesheet. As described in Section 12.0 of this report, the potential leakage due to degradation below 17 inches from the TTS would clearly be below allowable accident limits.

The findings in the Catawba 2 and Vogtle 1 SG tubes present three distinct issues with regard to the SG tubes at the Byron 2 and Braidwood 2 plants:

- 1) indications in internal bulges within the tubesheet,
- 2) indications at the elevation of the tack expansion transition, and
- 3) indications in the tube-to-tubesheet welds, including some extending into the tube.

The scope of this document is to: a) address the applicable requirements, including the original design basis, Reference 7, and regulatory issues, Reference 8, and b) provide analysis support for technical arguments to limit inspection of the tubesheet region to an area above which degradation could result in potentially not meeting the SG performance criteria, i.e., the depths specified in Section 7.0 of this report. The application of an H* type of justification to limit the inspection and repair extent of the tubes requires a redefinition of the primary-to-secondary pressure boundary for plants with hydraulically expanded tube-to-tubesheet joints for which a license amendment must be granted by the NRC for implementation. A similar Technical Specification change was approved, on a one-time basis, to limit inspections of the Braidwood 2 SGs during the spring 2005 inspection campaign in April 2005, Reference 9. A similar change has been requested for Byron 2 for use in the fall 2005 inspection campaign and is currently undergoing NRC review." This report was prepared to facilitate the approval of a modification of the H* criteria to justify the RPC exclusion zone to the portion of the tube below 17 inches from the top of the tubesheet and to provide the necessary information for a NRC staff review of the technical basis for that request.

It should be specifically noted that although the terminology of "H*" is used extensively throughout this document, Exelon is not attempting to license H*, but to use the H* criteria in order to support justification of a limited tube inspection extent from the top of the hot leg side of the tubesheet to a depth of 17 inches. Therefore, degradation below the top 17 inches of the tube within the tubesheet can remain in service since it is demonstrated herein to not be safety significant.

The development of the H* criteria involved consideration of the performance criteria for the operation of the SG tubes as delineated in NEI 97-06, Revision 1, Reference 10, and draft RG 1.121, Reference 11. The bases for the performance criteria are the demonstration of both structural and leakage integrity during normal operation and postulated accident conditions. The structural analyses using the H* criteria regarding the efficacy of the tube-to-tubesheet joint, and leak rate analyses based on empirical data and computer code modeling of the leakage from tubes postulated to be cracked 100% throughwall within the tubesheet are discussed in this report. The structural model was based on standard analysis techniques and finite element models as used for the original design of the SGs and documented in numerous submittals for the application of criteria to deal with tube indications within the tubesheet of other models of Westinghouse designed SGs with tube-to-tubesheet joints fabricated by other techniques, e.g., explosive expansion.

All full depth expanded tube-to-tubesheet joints in Westinghouse-designed SGs have a residual radial preload between the tube and the tubesheet. Early vintage SGs involved hard rolling which resulted in the largest magnitude of the residual interface pressure. Hard rolling was replaced by explosive expansion which resulted in a reduced magnitude of the residual interface pressure. Finally, hydraulic expansion replaced explosive expansion for the installation of SG tubes, resulting in a further reduction in the residual interface pressure. In general, it was found that the leak rate through the joints in hard rolled tubes, if any, is insignificant. Testing demonstrated that the leak rate resistance of explosively expanded tubes was not as great and prediction methods based on empirical data to support theoretical models were developed to deal with the potential for leakage. The same approach was followed to develop a prediction methodology for hydraulically expanded tubes. However, the model has been under review since its inception, with the intent of verifying its accuracy because it involved analytically combining the results from independent tests of leak rate through cracks with the leak rate through the tube-to-tubesheet crevice. The H* model for leak rate is such a model and its review could be time consuming since it has not been previously reviewed by the NRC staff. An alternative approach was developed for application at Braidwood 2 for the spring 2005 outage and Byron 2 for the fall 2005 outage based on engineering expectations of potential differences in the leak rate between normal operation and postulated accident conditions based on a first principles approach to the engineering. However, there are no technical reasons why the use of the alternate methodology should be limited to a single application at either plant site.

A summary of the evaluation is provided in Section 2.0 of this report. The historical background and design requirements for the tube-to-tubesheet joint are discussed in Sections 3.0 and 4.0 respectively. Section 5.0 addresses plant operating conditions at Byron 2 and Braidwood 2. Section 6.0 discusses the tube pullout and leakage test programs that are applicable to the Model D5 SGs at Byron 2/Braidwood 2. A summary of the conclusions from the structural analysis of the joint is provided in Section 7.0, the leak rate analysis in Section 8.0, a review of the qualitative arguments used by the NRC Staff for the tube joint inspection length approved for Braidwood Unit 2 is discussed in Section 9.0, dispositioning of cracked tubes inadvertently found below the

inspection distance is discussed in Section 10.0, conclusions from the structural and leak rate evaluations are provided in Section 11.0, and recommended tube inspection plans are contained in Section 12.0 of this report.

SG - 2A +Point Indications Within the Tubesheet

Catawba EOC13 DDP D5

E 1 INDICATION WITHIN 0.25" OF HOT LEG TUBE END
 ■ 66 PLUGGED TUBE

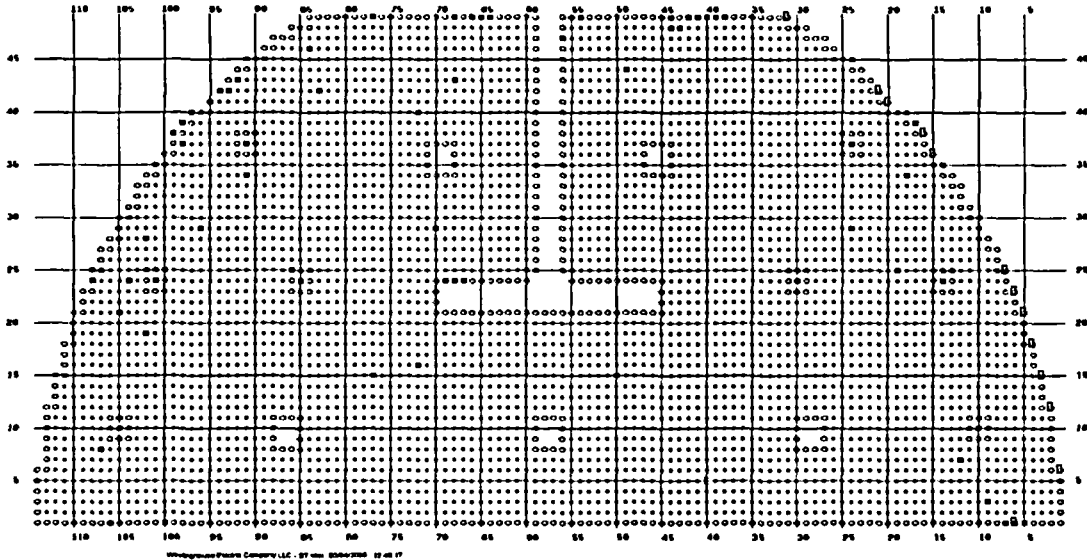


Figure 1-1. Distribution of Indications in SG A at Catawba 2

SG - 2B +Point Indications Within the Tubesheet

Catawba EOC13 DDP D5

Z 1 MULTIPLE INDICATIONS AT APPROXIMATELY 7" BELOW HOT LEG TOP OF TUBESHEET
 W 1 INDICATIONS WITHIN 0.25" AND BETWEEN 0.26" AND 0.80" OF HOT LEG TUBE END
 R 0 INDICATION BETWEEN 0.26" AND 0.80" OF HOT LEG TUBE END
 E 102 INDICATION WITHIN 0.25" OF HOT LEG TUBE END
 ■ 58 PLUGGED TUBE

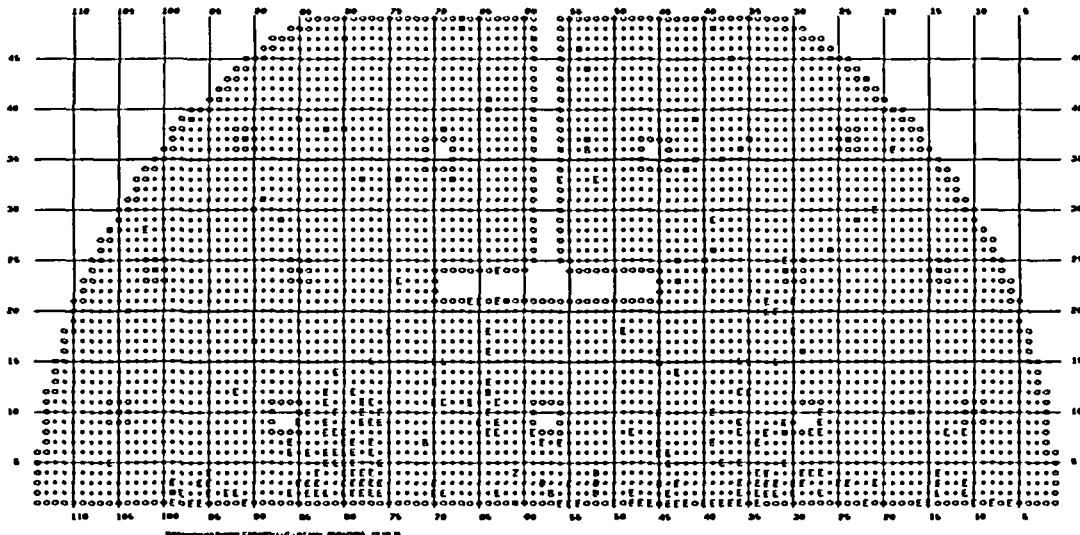


Figure 1-2. Distribution of Indications in SG B at Catawba 2

SG - 2D +Point Indications Within the Tubesheet

Catawba EOC13 DOPD5

E 7 INDICATION WITHIN 0.25" OF
HOT LEG TUBE END

■ 05 PLUGGED TUBE

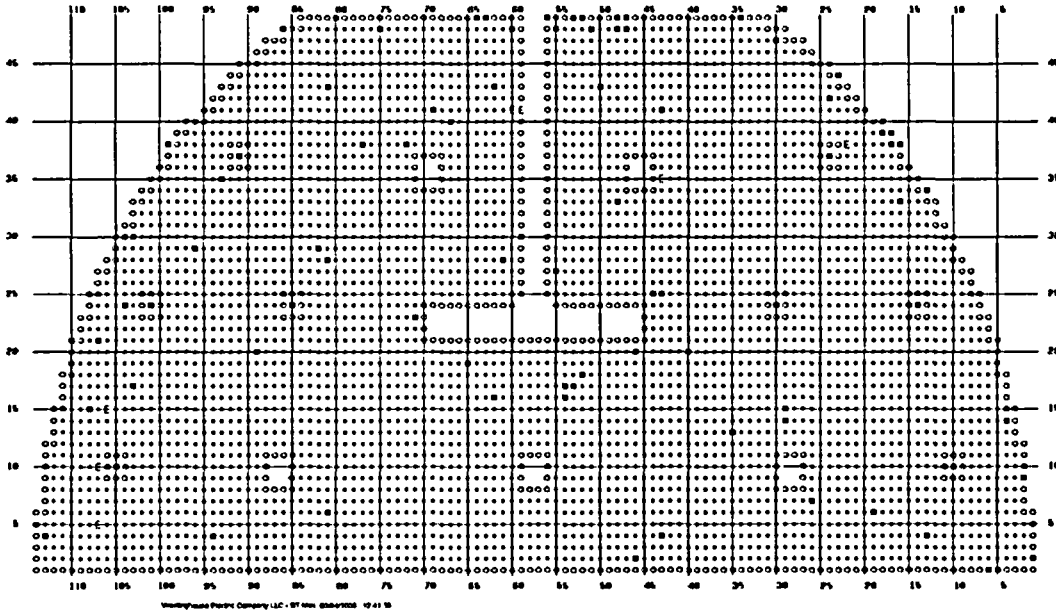


Figure 1-3. Distribution of Indications in SG D at Catawba 2

2.0 Summary Discussion

Evaluations were performed to assess the need for special purpose NDE probe examinations, e.g., RPC, of the SG tubes region within the tubesheet at the Byron 2 and Braidwood 2 power plants. The conclusions from the evaluation are that a 20% sample of the tube in each SG could be performed to at least the minimum depths of 2.9 inches in Zone A, 6.0 inches in Zone B and 8.6 inches in Zone C as identified in Section 7.0 of this report, to ensure structural integrity. Exelon has decided to perform, on a permanent basis, sampling RPC inspections to a depth of 17 inches below the top of the tubesheet for the Braidwood 2 SGs and Byron 2 in order to assure that the SLB leakage requirements in addition to the structural requirements are met.

It is noted that the above inspection recommendation excludes the region of the tube referred to as the tack expansion or the tack expansion transition. In addition, consideration was given to the need to perform inspections of the tube-to-tubesheet weld in spite of the fact that the weld is specifically not part of the tube in the sense of the plant technical specification, see Reference 2. With regard to the latter two regions of the primary-to-secondary pressure boundary in accord with the original design of the SGs, it is concluded that there is no need to inspect either the tack expansion, its transition, or the tube-to tubesheet welds for degradation because the tube in these regions has been shown to meet structural and leak rate criteria regardless of the level of degradation. Furthermore, it could also be concluded that for some of the tubes, depending on radial location in the tubesheet, there is not a need to inspect the region of the tube below the neutral plane of the tubesheet, roughly 11 inches below the top. The results from the evaluations performed as described herein demonstrate that the inspection of the tube within a nominal 4.23 inches of the tube-to-tubesheet weld and of the weld is not necessary for structural adequacy of the SG during normal operation or during postulated faulted conditions, nor for the demonstration of compliance with leak rate limits during postulated faulted events.

In summary:

- The structural integrity requirements of NEI 97-06, Reference 10, and draft RG 1.121, Reference 11, are met by sound tube engagement lengths ranging from 2.95 to 8.61 inches from the top of the tubesheet, thus the region of the tube below those elevations, including the tube-to-tubesheet weld is not needed for structural integrity during normal operation or accident conditions.
- NEI 97-06, Reference 10, defines the tube as extending from the tube-to-tubesheet weld at the tube inlet to the tube-to-tubesheet weld at the tube outlet, but specifically excludes the tube-to-tubesheet weld from the definition of the tube. The acceptance of the definition by the NRC staff was recorded in the Federal Register on March 2, 2005, Reference 12.
- The welds were originally designed and analyzed as primary pressure boundary in accordance with the requirements of Section III of the 1971 edition of the ASME Code,

Summer 1972 Addenda and selected paragraphs of the Winter 1974 Addenda, Reference 7. The analyses are documented in References 13 and 14 for the Byron 2 and Braidwood 2 SGs respectively. The typical as-fabricated and the as-analyzed weld configurations are illustrated on Figure 2-1.

- Section XI of the ASME Code, Reference 15 (1971) through 16 (2004), deals with the inservice inspection of nuclear power plant components. The ASME Code specifically recognizes that the SG tubes are under the purview of the NRC through the implementation of the requirements of the Technical Specifications as part of the plant operating license.

The hydraulically expanded tube-to-tubesheet joints in Model D5 SGs are not leak-tight without the tube end weld and considerations were also made with regard to the potential for primary-to-secondary leakage during postulated faulted conditions. However, the leak rate during postulated accident conditions would be expected to be less than that during normal operation for indications near the bottom of the tubesheet (including indications in the tube end welds) based on the observation that while the driving pressure increases by about a factor of two, the flow resistance increase associated with an increase in the tube-to-tubesheet contact pressure can be up to a factor of 3, Reference 5. While such a decrease in the leak rate is rationally expected, the postulated accident leak rate could conservatively be taken to be bounded by twice the normal operating leak rate if the increase in contact pressure is ignored. Since normal operating leakage is limited to less than 0.1 gpm, the attendant accident condition leak rate, assuming all leakage to be from lower tubesheet indications, would be bounded by 0.2 gpm. Therefore, the leak rate under normal operating conditions could exceed its allowed value before the accident condition leak rate would be expected to exceed its allowed value. This approach is termed an application of the "bellwether principle." Additionally, the accident analysis assumption of 0.5 gpm (room temperature) primary to secondary leakage in the affected SG for a postulated SLB for Byron Unit 2/Braidwood Unit 2 is greater than the bounding leak rate of 0.2 gpm. This assessment also envelopes postulated circumferential cracking of the tube or the tube-to-tubesheet weld that is 100% deep by 360° in extent because it is based on the premise that no weld is present.

Based on the information summarized above, no inspection of the tube-to-tubesheet welds, tack roll region or bulges below the distance determined to have the potential for safety significance as specified in Reference 5, i.e., the H* depths, would be considered to be the minimum distance to be necessary to assure compliance with the structural requirements for the SGs. In addition, based on the results from consideration of application of the bellwether principle regarding potential leakage during postulated accident conditions, the planned inspection to a depth of 17 inches below the top of the tubesheet is conservative and justified.

The selection of a depth of 17 inches obviates the need to consider the location of the tube expansion transition below the TTS, usually bounded by a length of about 0.3 inches. For structural purposes, the value of 17 inches greatly exceeds the engagement lengths determined

from the analysis documented in Reference 5. The application of the bellwether approach to the leak rate analysis as described in Section 8.1 of this report negates the need to consider specific distances from the TTS and relies only on the magnitude of the contact pressure in the vicinity of the tube above 17 inches below the TTS.

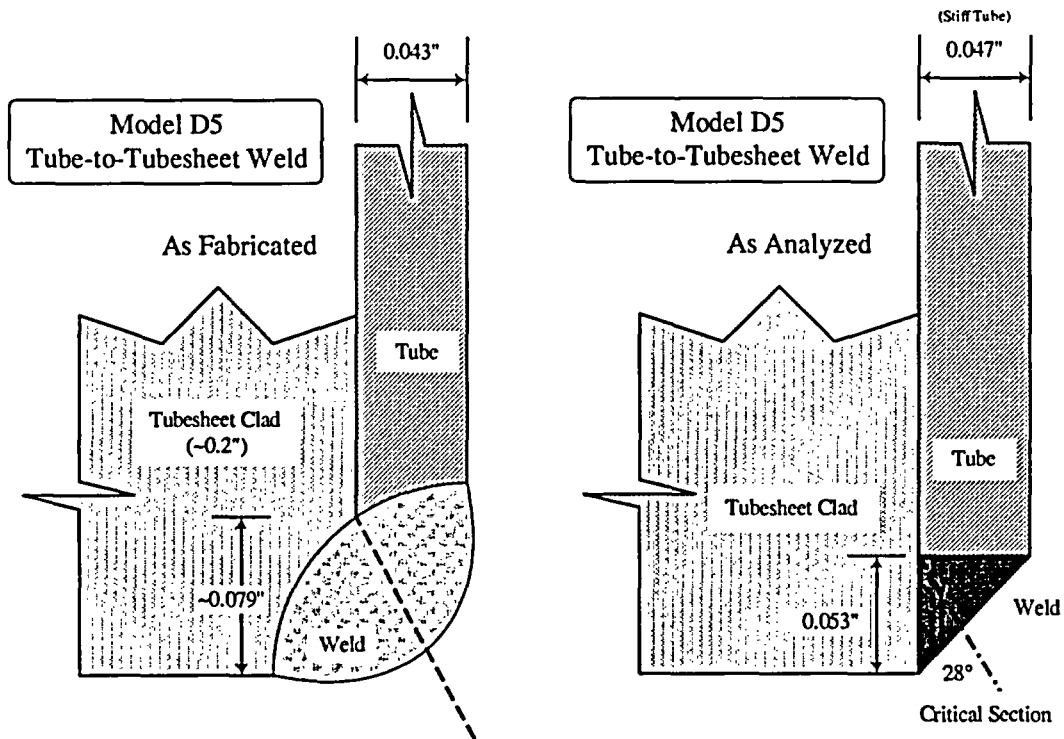


Figure 2-1. As-Fabricated & Analyzed Tube-to-Tubesheet Welds

3.0 Historical Background Regarding Tube Indications in the Tubesheet

There has been extensive experience associated with the operation of SGs wherein it was believed, based on NDE, that throughwall tube indications were present within the tubesheet. The installation of the SG tubes usually involves the development of a short interference fit, referred to as the tack expansion, at the bottom of the tubesheet. The tack expansion was usually effected by hard rolling through October of 1979 and thereafter, in most instances, by the Poisson expansion of a urethane plug inserted into the tube end and compressed in the axial direction. The rolling process by its very nature is considered to be more aggressive with regard to metalworking at the inside surface of the tube and would be expected to lead to higher residual surface stresses. It is believed that the rolling process was used during fabrication of the Byron Unit 2 SGs, while the urethane plug (Poisson) expansion process was used for those at Braidwood Unit 2. The tube-to-tubesheet weld was then performed to create the ASME Code pressure boundary between the tube and the tubesheet.¹

The development of the F* alternate repair criterion (ARC) in 1985-1986 for tubes hard rolled into the tubesheet was prompted by the desire to account for the inherent strength of the tube-to-tubesheet joint away from the weld and to allow tubes with degradation within the tubesheet to remain in service, Reference 17. The result of the development activity was the demonstration that the tube-to-tubesheet weld was superfluous with regard to the structural and leakage integrity of the rolled joint between the tube and the tubesheet. Once the plants were in operation, the structural and leakage resistance requirements for the joints were based on the plant Technical Specifications, and a means of demonstrating joint integrity that was acceptable to the NRC staff was delineated in Reference 11. License amendments were sought and granted for several plants with hard rolled tube-to-tubesheet joints to omit the inspection of the tube below a depth of about 1.5 inches from the top of the tubesheet. Similar criteria, designated as W*, were developed for explosively expanded tube-to-tubesheet joints in Westinghouse designed SGs in the 1991-1992 timeframe, Reference 18. The W* criteria were first applied to operating SGs in 1999 based on a generic evaluation for Model 51 SGs, Reference 19, and the subsequent safety evaluation by the NRC staff, Reference 20. However, the required engagement length to meet structural and leakage requirements was on the order of 4 to 6 inches because the explosively expanded joint does not have the same level of residual interference fit as that of a rolled joint. It is noted that the length of joint necessary to meet the structural requirements is not the same as, and is usually shorter than, that needed to meet the leakage integrity requirements.

The post-weld expansion of the tube into the tubesheet in the Byron 2 and Braidwood 2 SGs was effected by a hydraulic expansion of the tube instead of rolling or explosive expansion. The hydraulically formed joints do not exhibit the level of interference fit that is present in rolled or

¹ The actual weld is between the Alloy 600 tube and weld buttering, a.k.a. cladding, on the bottom of the carbon steel tubesheet.

explosively expanded joints, however, when the thermal and internal pressure expansion of the tube is considered during normal operation and postulated accident conditions, appropriate conclusions regarding the need for the weld similar to those for the other two types of joint can be made. Evaluations were performed in 1996 of the effect of tube-to-tubesheet weld damage that occurred from an object in the bowl of a SG with tube-to-tubesheet joints similar to those in the Byron 2 and Braidwood 2 SGs, on the structural and leakage integrity of the joint, Reference 21. It was concluded in that evaluation that the strength of the tube-to-tubesheet joint is sufficient to prevent pullout in accordance with the requirements of the performance criteria of Reference 10 and that a significant number of tubes could be damaged without violating the performance criterion related to the primary-to-secondary leak rate during postulated accident conditions.

4.0 Design Requirements for the Tube-to-Tubesheet Joint Region

This section provides a review of the applicable design and analysis requirements, including the ASME Code pre-service design requirements of Section III and the operational/maintenance requirements of Section XI. The following is the Westinghouse interpretation of the applicable analysis requirements and criteria for the condition of TEW cracking. Recommendations that include code requirements and the USNRC position as expressed in References 8 and 10. Reference 8 notes that:

“In accordance with Section III of the Code, the original design basis pressure boundary for the tube-to-tubesheet joint included the tube and tubesheet extending down to and including the tube-to-tubesheet weld. The criteria of Section III of the ASME Code constitute the “method of evaluation” for the design basis. These criteria provide a sufficient basis for evaluating the structural and leakage integrity of the original design basis joint. However, the criteria of Section III do not provide a sufficient basis by themselves for evaluating the structural and leakage integrity of a mechanical expansion joint consisting of a tube expanded against the tubesheet over some minimum embedment distance. If a licensee is redefining the design basis pressure boundary and is using a different method of evaluation to demonstrate the structural and leakage integrity of the revised pressure boundary, an analysis under 10 CFR 50.59 would determine whether a license amendment is required.”

The industry definition of Steam Generator Tubing excludes the tube-end weld from the pressure boundary as noted in NEI 97-06 (Reference 10):

“Steam generator tubing refers to the entire length of the tube, including the tube wall and any repairs to it, between the tube-to-tube sheet weld at the tube inlet and the tube-to-tube sheet weld at the tube outlet. The tube-to-tube sheet weld is not considered part of the tube.”

The NRC has indicated its concurrence with this definition, see, for example, Reference 12. In summary, from a non-technical viewpoint, no specific inspection of the tube-end welds would be required because:

1. The industry definition of the tube excludes the tube-end weld,
2. The ASME Code defers the judgment regarding the redefined pressure boundary to the licensing authority under 10CFR50.59,
3. The NRC has accepted this definition; therefore, by inference, may not consider cracked welds to be a safety issue on a level with that of cracked tubes, and

-
4. There is no qualified technique that can realistically be applied to determine if the tube-end welds are cracked.

However, based on the discussion of Information Notice 2005-09, Reference 2, it is clear that the NRC staff has concluded that “the findings at Catawba illustrate the importance of inspecting the parent tube adjacent to the weld and the weld itself for degradation.” The technical considerations documented herein obviate the need for consideration of any and all non-technical arguments.

5.0 Operating Conditions

Byron/Braidwood 2 is a four-loop plant with Model D5 steam generators; there are 4570 tubes in each SG. The design of these SGs includes Alloy 600 thermally treated tubing, full-depth hydraulically expanded tubesheet joints, and broached hole quatrefoil tube support plates constructed of stainless steel.

5.1 Bounding Operating Conditions

Values that bound the current Byron/Braidwood 2 steam generator thermal and hydraulic parameters during normal operation are tabulated below (Note: these values assume a 10% SG tube plugging level.):

Parameter Units		Bounding Operating Conditions (1)
Power – NSSS	MWt	3600.6
Reactor Vessel Outlet Temperature	°F	608.0
Reactor Coolant System Pressure	psig	2235
SG Steam Temperature	°F	519.8
SG Steam Pressure	psig	796

(1) Reference 22

5.2 Faulted Conditions

In addition to the RG 1.121 criteria, it is necessary to satisfy the updated final safety analysis report (UFSAR) accident condition assumptions for primary-to-secondary leak rates. Calculated primary-to-secondary side leak rate during postulated events should: 1) not exceed the total charging pump capacity of the primary coolant system, and 2) be such that the off-site radiological dose consequences do not exceed Title 10 of the Code of Federal Regulations (10 CFR) Part 100 guidelines.

The accident condition primary-to-secondary leakage must be limited to acceptable values established by plant specific UFSAR evaluations. The appropriate value for the Byron/Braidwood 2 SGs is 0.5 gpm (at room temperature) for the affected SG. Pressure differentials associated with a postulated accident condition event can result in leakage from a throughwall crack through the interface between a hydraulically expanded tube in the tubesheet and the tube hole surface. Therefore, a steam generator leakage evaluation for faulted conditions is provided in this report. The accidents that are affected by primary-to-secondary leakage are those that include, in the activity release and off-site dose calculation, modeling of leakage and secondary steam release to

the environment. Steamline break (SLB) is the limiting condition; the reasons that the SLB is limiting are: 1) the SLB primary-to-secondary leak rate in the faulted loop is assumed to be greater than the operating leak rate because of the sustained increase in differential pressure, and 2) leakage in the faulted steam generator is assumed to be released directly to the environment. For evaluating the radiological consequences due to a postulated SLB, the activity released from the affected SG (which is connected to the broken steam line) is released directly to the environment. The unaffected steam generators are assumed to continually discharge steam and entrained activity via the safety and relief valves up to the time when initiation of the RHR system can be accomplished. A 0.5 gpm primary-to-secondary leakage is assumed for the affected SG. The radiological consequences evaluated, based on meteorological conditions, assumed that all of this flow goes to the affected steam generator. With this level of leakage, the resultant doses are well within the guideline values of 10 CFR 100.

6.0 Steam Generator Tube Leakage and Pullout Test Program Discussion

The test program, completed for Model D5 and Model F steam generator (Reference 5) had two purposes:

1. To determine the [

a.

b.

2.

]a.c.e.

6.1 Model F Tube Joint Leakage Resistance Program

A total of [

]a.c.e

The lower bound leakage resistance distribution for the collars with the nominal tubesheet hole diameter was used in the present leakage evaluation. This lower bound leakage resistance was made using data for the test conditions shown in the table below.

Table 6-1
Model F Leak Test Program Matrix

a.c.c

6.1.1 Test Sample Configuration

The intent of the test samples was to model key features of the Model F tube-to-tubesheet joint for []^{a.c.c}. The following hardware was used:

6.1.1.1 Tubesheet Simulant (Collar)

The collar simulated the circumferential stiffness of a Model F tubesheet unit cell, utilizing an appropriate outside diameter of approximately []

]a.c.c.

6.1.1.2 Tubing

The yield strength for the SG Alloy 600 tubing in the plants ranges between []^{a.c.c.}. The Alloy 600 tubing used for these tests was from a certified heat and lot conforming to ASME SB163, Section III Class 1. It was obtained from a Quality Systems-controlled Storeroom. .

6.1.1.3 Test Sample Design Configuration

The intent of the leakage portion of the test program was to determine the leakage resistance of simulated Model F tube-to-tubesheet joints, disregarding the effect of the tube-to-tubesheet weld and the []^{a.c.c.}.

(These welds were an artifact of the test design and did not affect the test condition because they made no contribution to hydraulic resistance from the tube-to-tubesheet weld or the tube tacking operation.)

6.1.1.4 Test Sample Assembly

6.1.1.4.1 Tube Tack Expansion Operation

The steam generator factory tubing drawing specifies a []^{a.c.c.}, to facilitate the tube weld to the cladding on the tubesheet face and it was omitted from the test.

6.1.1.4.2 Tube Hydraulic Expansion

The hydraulic expansion pressure range for the Model F steam generators was approximately []

] ^{a.c.c}. This value conservatively bounds the lower expansion pressure limit used for the Model F steam generators.

The tube expansion tool used in the factory consisted of a pair of seals, spaced by a tie rod between them. The hydraulically expanded zone was positioned relative to the lower surface of the tubesheet, overlapping the upper end of the tack expanded region. It extended to within a short distance of the upper surface of the tubesheet. This produced a hydraulically expanded length of approximately [] ^{a.c.c} inch nominal tubesheet depth.

The majority of the test samples were fabricated using []

] ^{a.c.c}. These samples are described as “Segmented Expansion” types. A tube expansion schematic is shown in Figure 6-2.

A small group of the test samples were fabricated using a [] ^{a.c.c} tool which was fabricated expressly for these tests. These samples were described as “Full Depth Expansion” types. The expansion method with regard to the segmented or full length aspect does not have a bearing on the test results.

6.2 Model D5 Tube Joint Leakage Resistance Program

A total of []

] ^{a.c.c}

The lower bound leakage resistance distribution for the collars with the nominal tubesheet hole diameter was used in the present leakage evaluation. This lower bound leakage resistance was made using data for the test conditions shown in the Table 6-2 below combined with the Model F leak test results discussed in Section 6.1.

6.2.1 Test Sample Configuration

The intent of the test samples was to model key features of the Model D5 tube-to-tubesheet joint for []^{a.c.c.}. The following hardware was used:

6.2.1.1 Tubesheet Simulant (Collar)

The collar simulated the circumferential stiffness of a Model D5 tubesheet unit cell, utilizing an appropriate outside diameter of approximately []^{a.c.c.}

6.2.1.2 Tubing

The average yield strength for the SG Alloy 600 tubing in the Model D plants is []^{a.c.c.}. The Alloy 600 tubing used for these tests was from heats conforming to ASME SB163, Section III Class 1. It was obtained from a Quality Systems-controlled Storeroom

6.2.1.3 Tube Sample Design, Fabrication and Test Set-Up

The intent of the leakage portion of the test program was to determine the leakage resistance of simulated Model D5 tube-to-tubesheet joints, disregarding the effect of the []^{a.c.c.}

Tube-to-tubesheet simulant samples of the Model D5 configuration were designed and fabricated. The steam generator factory tubing drawing specifies a []^{a.c.c.}

The hydraulic expansion pressure range for the Model D5 steam generators was []^{a.c.c.}. This value conservatively bounds the lower expansion pressure limit used for the Model D5 steam generators. Refer to Figure 6-3 for the details of the configuration for the leak test. The test equipment consisted of a make-up tank (MUT), primary water autoclave (AC1) and a secondary autoclave (AC2) connected by insulated pressure tubing. Two specimens were installed into the secondary autoclave to minimize setup time and variability across test runs. AC1 was run with

deoxygenated primary water containing specified amounts of boron, lithium and dissolved hydrogen. The primary chemistry conditions were controlled in the MUT and a pump and backpressure system allowed the primary water to re-circulate from the MUT to the AC1. The primary autoclave had the normal controls for heating, monitoring pressure and safety systems including rupture discs. Figure 6-4 shows the entire test system with key valves and pressure transducers identified. In addition to the normal controls for heating, monitoring pressure and maintaining safety, the secondary autoclave was outfitted with water cooled condensers that converted any steam escaping from the specimens into room temperature water. The pressure in the secondary side (in the main body of AC2), was monitored by pressure transducers. For most tests, the leakage was collected in a graduated cylinder on a digital balance connected to a computer so that the amount of water could be recorded as a function of time. For some normal operating tests, the leakage was calculated based on changes in the secondary side pressure. All relevant autoclave temperatures and pressures were recorded with an automatic data acquisition system at regular time intervals.

6.2.1.4 Test Sample Assembly

The assumption that pull-out resistance is distributed uniformly through the axial extent of the joint is an adequate technical approach. The pullout resistance is asymptotic to some large value, the form of the relation is one minus an exponential to a negative multiple of the length of engagement. For short engagement lengths, say up to 5 to 8 inches, the linear approximation is sufficient. Extrapolations to higher pullout resistance for longer lengths could be non-conservative except for the fact that the pullout strength of the shorter lengths exceed the structural performance criteria.

6.3 Model D5 Tube Joint Pullout Resistance Program

The Model D5 pullout test samples were fabricated with the same processes as used for the leakage test. Refer to Figure 6-5.

The tube expansion tool used in the program was a factory device, modified to achieve an expansion ranging of from three to seven inches.

6.4 Test Procedure

6.4.1 Model F Leakage Resistance Test

The testing reported herein was performed according to a test procedure which outlined two types of leak tests. The tests performed are described below.

6.4.1.1 Model F Elevated Temperature Primary-to-Secondary Leak Tests

For the Model F testing, elevated temperature primary-to-secondary side leak tests were performed using an [

] ^{a,c,e}.

These tests were performed following the room temperature primary-to-secondary side leak tests on the chosen samples. The test results showed a [

] ^{a,c,e}.

6.4.1.2 Model F Room Temperature Primary-to-Secondary Side Leak Tests

For the Model F testing, room temperature primary-to-secondary leak tests were performed on all test samples [

] ^{a,c,e}. These tests were performed following the elevated temperature primary-to-secondary side leak tests on the chosen samples.

6.4.2 Model D5 Leakage Tests

For the Model D5 testing, primary-to-secondary leak tests were performed on all test samples, using simulated primary water as a pressurizing medium. Refer to Figure 6-3 [

] ^{a.c.e}, to simulate a perforation of the tube wall due to corrosion cracking. All of the elevated temperature primary-to-secondary side leak tests were performed using an [] ^{a.c.e} as the pressurizing/leakage medium. In the case of 800 psi back pressure tests, the leakage was collected in the autoclave as it issued from the tube-to-collar crevice. In the remainder of the autoclave tests, the leakage was collected in the autoclave as it issued from the tube-to-collar crevice but it was piped to a condenser/cooler and weighed on an instrumented scale.

6.4.3 Model D5 Mechanical Loading Tests

Model D5 Hydraulic expansion joints of axial lengths of [

] ^{a.c.e}

Joint strength, based on the recorded load-deflection curve is typically taken as anywhere from the [“

] ^{a.c.e}

Generally, but not always, the larger-deflection load value is greater than the knee value. In this program, it was planned to use [] ^{a.c.e} a.k.a. deflection, to obtain the input information for calculation of the H* values for the plants. The pullout load from these plots simply provides one of the inputs used to calculate H*. The other variables include tubesheet bending (causing the tubesheet hole to dilate and/or contract depending on the distance of a certain point below the tubesheet top), the thermal growth mismatch effect (owing to the differential thermal growth between the tube (Alloy 600) and the tubesheet (steel) and the “differential pressure tightening” of the tube within the tubesheet.

The load-displacement curves for 3 of the 12 tube-to-simulant tests are shown below in Figure 6-7. The first digit of the XX portion of the D5H-XX-Y title refers to the nominal temperature at which the test was run, “6” for 600°F, etc. The second digit refers to the nominal axial length of the hydraulic expansion, for instance, “5” for the 5 inch-long joint. (The “Y” portion is the number of the sample at the given temperature and expansion length.)

Examination of the plots shows that using the maximum load within the displacement of [] ^{a.c.e}

The force resisting tube pullout from the tubesheet in the plant, acting on a length of a tube between elevations h_1 and h_2 , reckoned from a convenient elevation such as the tubesheet secondary side face, is shown in Section 7.2 of this report.

6.5 Test Summary

6.5.1 Leak Test Results

6.5.1.1 Model F Leak Test Results

The leak tests on segmented expansion collars averaged [

] ^{a.c.c}. (As a point of reference, there are approximately 75,000 drops in one gallon.) Leakage data were also recorded at room temperature conditions to provide input for the low contact pressure portion of the flow loss coefficient-versus-contact pressure correlation.

6.5.1.2 Model D5 Leak Tests

The leakage rates for the Model D5 600°F normal operating and accident pressure differential conditions were similar to the respective Model F values. Leakage ranged from [

] ^{a.c.c} Leakage data were also recorded at room temperature conditions to provide input for the low contact pressure portion of the flow loss coefficient-versus-contact pressure correlation.

6.5.1.3 Leak Loss Coefficient Determination Discussion

In order to produce a plot of loss coefficient (K) versus contact pressure (CP or P) for the Model D5 and Model F steam generators, loss coefficients for the Model D5 steam generators were calculated using the Darcy flow approximation and elevated temperature Model F and Model D5 test data produced internally by Westinghouse. The Model F data are taken from a previous H* analysis that was performed for the Model F steam generators. See Figure 6-6.

6.5.2 Model D5 Tube Pullout Test Results

Mechanical loading, [

Section 7.0 of this report.

] ^{a.c.c} The results are analyzed in

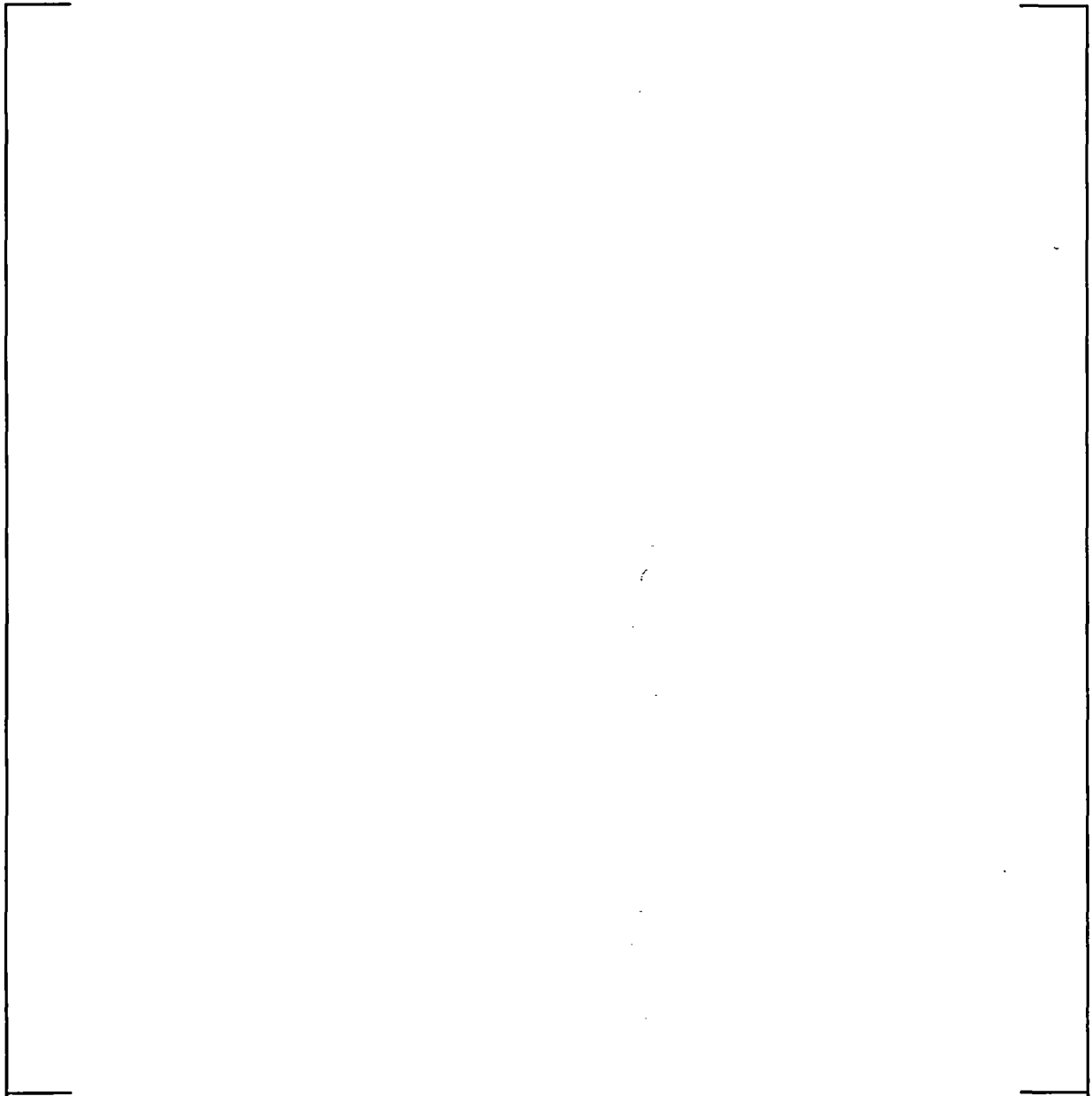


Figure 6-1.
Model F Leakage Test Schematic

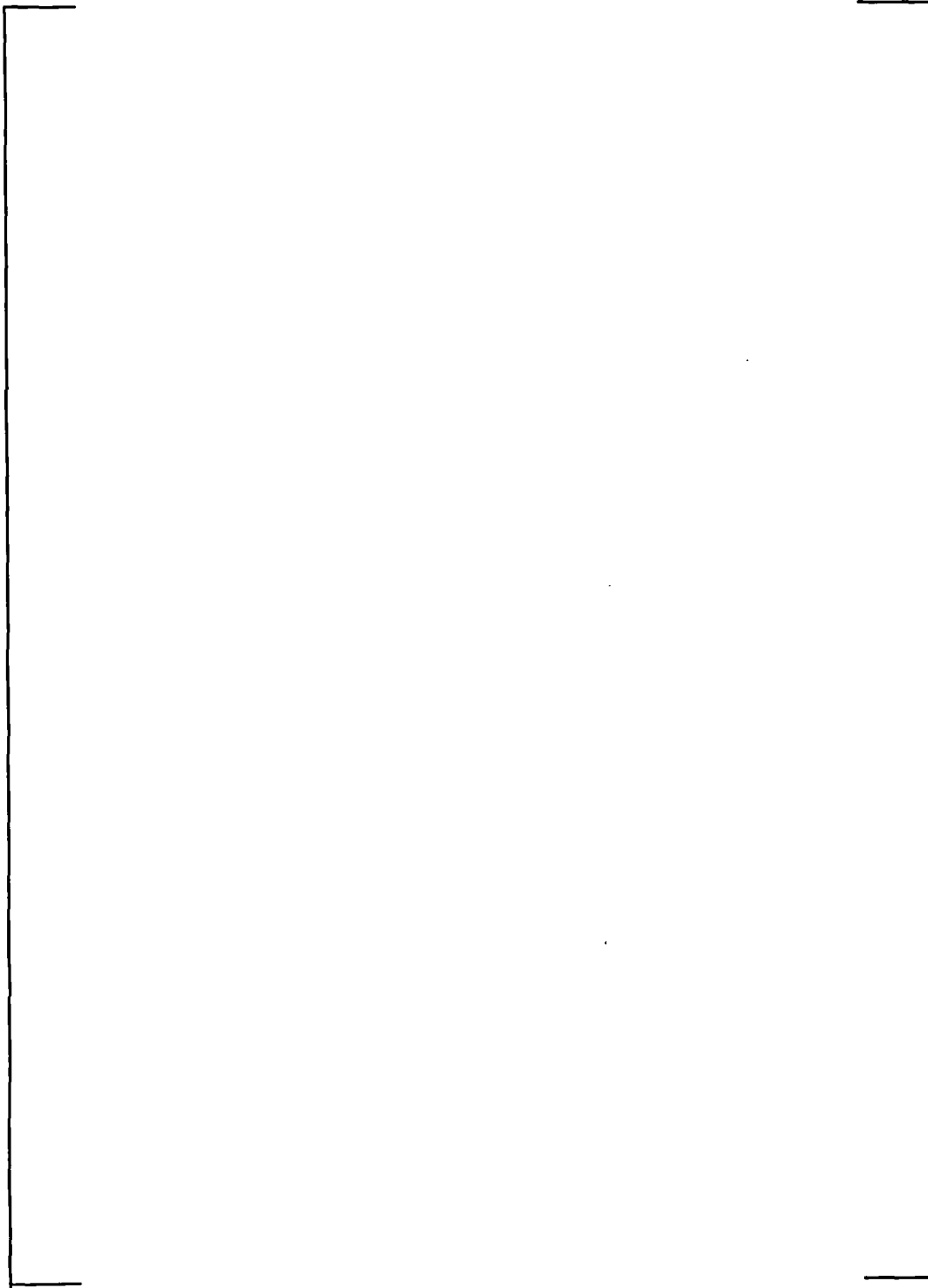


Figure 6-2.
Model F Tube Hydraulic Expansion Process Schematic

a, c. e



Figure 6-3.
Model D5 Tube Joint Sample Leakage Test Configuration

a, c, e

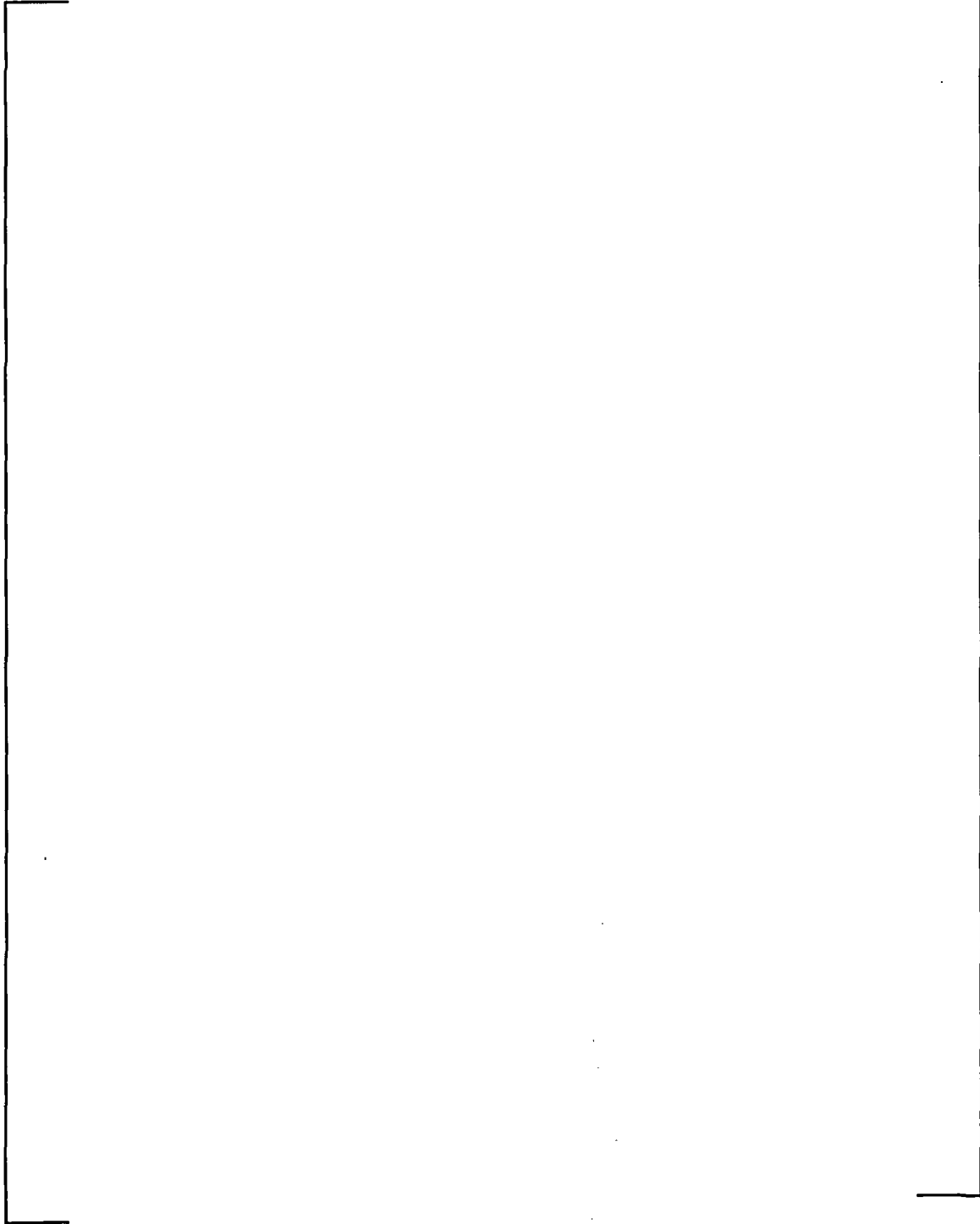


Figure 6-4.
Schematic for the Test Autoclave Systems for Leak Rate Testing



Figure 6-5.
Model D5 Tube Joint Sample Pullout Test Configuration



Figure 6-6.
Flow Resistance Curve

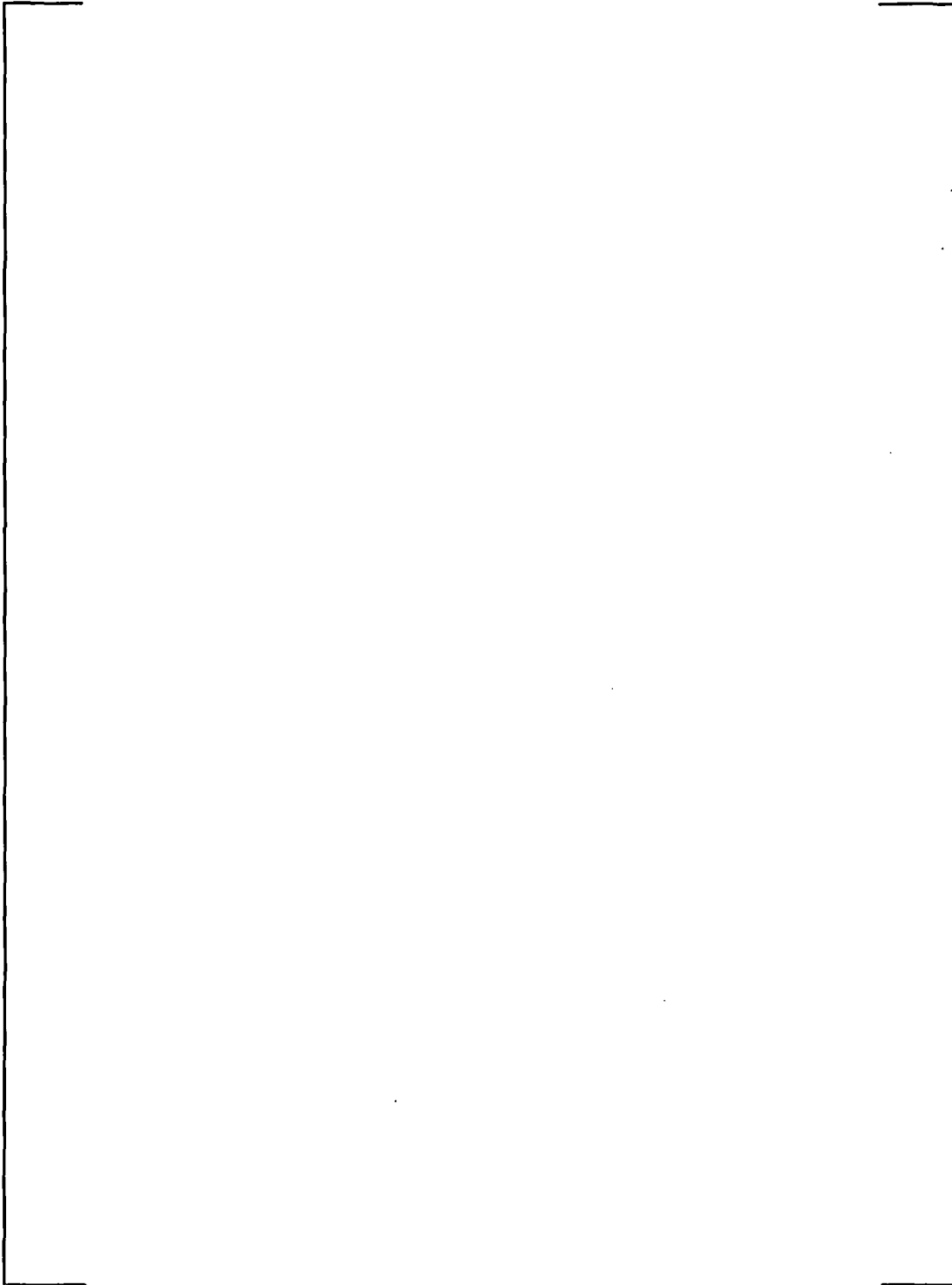


Figure 6-7.

Model D5 Pullout Test Data from Several Samples

Note: Sample test temperature and length of hydraulic expansion are identified in a text box at the upper left hand corner above the plot area of each load-displacement curve. The code is explained in Section 6.4.3 of this report.

7.0 Structural Analysis of Tube-to-Tubesheet Joint

This section summarizes the structural aspects and analysis of the entire tube-to-tubesheet joint region. The tube end weld was originally designed as a pressure boundary structural element in accordance with the requirements of Section III of the ASME (American Society of Mechanical Engineers) Boiler and Pressure Vessel Code, Reference 7. The construction code for the Byron and Braidwood Unit 2 SGs was the 1971 edition with the Summer 1972 and some paragraphs of the Winter 1974 addenda. This means that there were no strength considerations made with regard to the expansion joint between the tube and the tubesheet, including the tack expansion regardless of whether it was achieved by rolling or Poisson expansion of a urethane plug.

An extensive empirical and analytical evaluation of the structural capability of the as-installed tube-to-tubesheet joints based on considering the weld to be absent has been performed specifically for the Byron 2 and Braidwood 2 Model D5 SGs and the results are reported below. Typical Model D5 hydraulic expansion joints with lengths comparable to those being proposed in below for limiting RPC examination were tested for pullout resistance strength at temperatures ranging from 70 to 600°F. The results of the tests coupled with those from finite element evaluations of the effects of temperature and primary-to-secondary pressure on the tube-to-tubesheet interface loads have been used to demonstrate that engagement lengths of approximately 3 to 8.6 inches were sufficient to equilibrate the axial loads resulting from consideration of 3 times the normal operating and 1.4 times the limiting accident condition pressure differences. The variation in required engagement length is a function of tube location, i.e., row and column, and decreases away from the center of the SG where the maximum value applies. The tubesheet bows, i.e., deforms, upward from the primary-to-secondary pressure difference and results in the tube holes becoming dilated above the neutral plane of the tubesheet, which is a little below the mid-plane because of the effect of the tensile membrane stress from the pressure loading. The amount of dilation is a maximum very near the radial center of the tubesheet (restricted by the divider plate) and diminishes with increasing radius outward. Moreover, the tube-to-tubesheet joint becomes tighter below the neutral axis and is a maximum at the bottom of the tubesheet². In conclusion, the need for the weld is obviated by the interference fit between the tube and the tubesheet. Axial loads are not transmitted to the portion of the tube below the H* distance during operation or faulted conditions, by factors of safety of at least 3 and 1.4 respectively, including postulated loss of coolant accidents (LOCA), and inspection of the tube below the H* distance including the tube-to-tubesheet weld is not technically necessary. Also, if the expansion joint were not present, there would be no effect on the strength of the weld from axial cracks, and tubes with circumferential cracks up to about 180° by 100% deep would have sufficient strength to meet the nominal ASME Code structural requirements, based on the margins of safety reported in References 13 and 14, and the requirements of RG 1.121, Reference 11.

An examination of Tables 7-7 through 7-11 illustrates that the holding power of the tube-to-tubesheet joint in the vicinity of the maximum inspection depth of 17 inches is much greater than at

the top of the tubesheet in the range of the originally developed H^* . Note that the radii reported in these tables were picked to conservatively represent the entire radial zones of consideration as defined on Figure 7-1. For example, Zone C has a maximum radius of 34.4 inches. However, in order to establish H^* values that were conservative throughout the zone, the tube location for which the analysis results were most severe above the neutral axis were reported, i.e., those values calculated for a tube at a radius of 4.08 inches. The values are everywhere conservative above the neutral surface of the tubesheet for tubes in Zone C. Likewise for tubes in Zone B under the heading 49.035 inches where the basis for the calculation was a tube at a radius of 34.4 inches. The purpose of this discussion is to illustrate the extreme conservatism associated with the holding power of the joint below the neutral surface of the tubesheet, and to identify the proper tube radii for consideration. In the center of the tubesheet the incremental holding strength in the 4.9 inch range from 12 to 16.9 inches below the top of the tubesheet is about 1191 lbf per inch during normal operation. The performance criterion for $3\Delta P$ is met by the first 1.7 inch of engagement above 17 inches. At a radius of 59 inches the corresponding length of engagement needed is about 2.1 inches. The corresponding values for steam line break conditions are 1.07 and 1.69 inches at radii of 4.08 and 58.8 inches respectively. In other words, while a value of 8.6 inches was determined for H^* from the top of the tubesheet, a length of 1.7 to 1.85 inches would be sufficient at the bottom of the inspection length, where the latter value corresponds to a radius of 34.4 inches from the center of the tubesheet, the maximum extent of Zone C.

7.1 Evaluation of Tubesheet Deflection Effects for Tube-to-Tubesheet Contact Pressure

A finite element model was developed for the Model D5 tubesheet, channel head, and shell region to determine the tubesheet hole dilations in the Byron/Braidwood steam generators. [

] ^{a.c.e}

loads in the tube.

7.1.1 Material Properties and Tubesheet Equivalent Properties

The tubes in the Byron 2 and Braidwood 2 SGs were fabricated of A600TT material. Summaries of the applicable mechanical and thermal properties for the tube material are provided in Table 7-1. The tubesheets were fabricated from SA-508, Class 2a, material for which the properties are listed in Table 7-2. The shell material is SA-533 Grade A Class 2, and its properties are in Table 7-3. Finally, the channel head material is SA-216 Grade WCC, and its properties are in Table 7-4. The material properties are from Reference 25, and match the properties listed in the ASME Code.

The perforated tubesheet in the Model D5 channel head assembly is treated as an equivalent solid plate in the global finite element analysis. An accurate model of the overall plate behavior was

² There is a small reversal of the bending stress beyond a radius of about 55 inches because the support ring prevents rotation and the hole dilation is at the bottom of the tubesheet.

achieved by using the concept of an equivalent elastic material with anisotropic properties. For square tubesheet hole patterns, the equivalent material properties depend on the orientation of loading with respect to the symmetry axes of the pattern. An accurate approximation was developed [Reference 26], where energy principles were used to derive effective average isotropic elasticity matrix coefficients for the in-plane loading. The average isotropic stiffness formulation gives results that are consistent with those using the Minimum Potential Energy Theorem, and the elasticity problem thus becomes axisymmetric. The solution for strains is sufficiently accurate for design purposes, except in the case of very small ligament efficiencies, which are not of issue for the evaluation of the SG tubesheet.

The stress-strain relations for the axisymmetric perforated part of the tubesheet are given by:

$$\begin{bmatrix} \sigma_R^* \\ \sigma_\theta^* \\ \sigma_z^* \\ \tau_{RZ}^* \end{bmatrix} = \begin{bmatrix} D_{11} & D_{12} & D_{13} & 0 \\ D_{21} & D_{22} & D_{23} & 0 \\ D_{31} & D_{32} & D_{33} & 0 \\ 0 & 0 & 0 & D_{44} \end{bmatrix} \begin{bmatrix} \epsilon_R^* \\ \epsilon_\theta^* \\ \epsilon_z^* \\ \gamma_{RZ}^* \end{bmatrix}$$

with the elasticity coefficients are calculated as:

$$\begin{aligned} D_{11} = D_{22} &= \frac{\bar{E}_p^*}{f(1+\bar{\nu}_p^*)} \left[1 - \frac{\bar{E}_p^*}{E_z^*} \nu^2 \right] + \frac{1}{2} \left[\bar{G}_p^* - \frac{\bar{E}_p^*}{2(1+\bar{\nu}_p^*)} \right] \\ D_{21} = D_{12} &= \frac{\bar{E}_p^*}{f(1+\bar{\nu}_p^*)} \left[\bar{\nu}_p^* + \frac{\bar{E}_p^*}{E_z^*} \nu^2 \right] - \frac{1}{2} \left[\bar{G}_p^* - \frac{\bar{E}_p^*}{2(1+\bar{\nu}_p^*)} \right] \\ D_{13} = D_{23} = D_{31} = D_{32} &= \frac{\bar{E}_p^* \nu}{f} \\ D_{33} &= \frac{E_z^* (1 - \bar{\nu}_p^*)}{f} \text{ and } D_{44} = \bar{G}_z^* \\ \text{where } f &= 1 - \bar{\nu}_p^* - 2 \frac{\bar{E}_p^*}{E_z^*} \nu^2 \text{ and } \bar{G}_p^* = \frac{\bar{E}_d^*}{2(1+\bar{\nu}_d^*)}. \end{aligned}$$

Here,

- \bar{E}_p^* = Effective elastic modulus for in-plane loading in the pitch direction,
- E_z^* = Effective elastic modulus for loading in the thickness direction,
- $\bar{\nu}_p^*$ = Effective Poisson's ratio for in-plane loading in the pitch direction,
- \bar{G}_p^* = Effective shear modulus for in-plane loading in the pitch direction,
- \bar{G}_z^* = Effective modulus for transverse shear loading,
- \bar{E}_d^* = Effective elastic modulus for in-plane loading in the diagonal direction,
- $\bar{\nu}_d^*$ = Effective Poisson's ratio for in-plane loading in the diagonal direction, and,
- ν = Poisson's ratio for the solid material.

The tubesheet is a thick plate and the application of the pressure load results in a generalized plane strain condition. The pitch of the square, perforated hole pattern is 1.0625 inches and nominal hole diameters are 0.764 inch. The ID of the tube after expansion into the tubesheet is taken to be 0.67886 inch based on an assumption of 1% thinning during installation. Equivalent properties of the tubesheet are calculated without taking credit for the stiffening effect of the tubes.

$$\text{Ligament Efficiency, } \eta = \frac{h_{\text{nominal}}}{P_{\text{nominal}}}$$

where: $h_{\text{nominal}} = P_{\text{nominal}} - d_{\text{maximum}}$
 $P_{\text{nominal}} = 1.0625$ inches, the pitch of the square hole pattern
 $d_{\text{maximum}} = .764$ inches, the tube hole diameter

Therefore, $h_{\text{nominal}} = 0.2985$ inches (1.0625-0.764), and $\eta = 0.2809$ when the tubes are not included. From Slot, Reference 27, the in-plane mechanical properties for Poisson's ratio of 0.3 are:

Property	Value
\bar{E}_p^* / E	= 0.3992
$\bar{\nu}_p^*$	= 0.1636
\bar{G}_p^* / G	= 0.1674
E_z^* / E	= 0.5935
G_z^* / G	= 0.4189

where the subscripts p and d refer to the pitch and diagonal directions, respectively. These values are substituted into the expressions for the anisotropic elasticity coefficients given previously. In the global model, the X-axis corresponds to the radial direction, the Y-axis to the vertical or tubesheet thickness direction, and the Z-axis to the hoop direction. The directions assumed in the derivation of the elasticity coefficients were X- and Y-axes in the plane of the tubesheet and the Z-axis through the thickness. In addition, the order of the stress components in the WECAN/Plus (Reference 28) elements used for the global model is σ_{xx} , σ_{yy} , τ_{xy} , and σ_{zz} . The mapping between the Reference 26 equations and WECAN/+ is therefore:

Coordinate Mapping	
Reference 26	WECAN/+
1	1
2	4
3	2
4	3

Table 7-2 gives the modulus of elasticity, E, of the tubesheet material at various temperatures. Using the equivalent property ratios calculated above in the equations presented at the beginning of this section gives the elasticity coefficients for the equivalent solid plate in the perforated region of

the tubesheet. These are listed in Table A.5 for the tubesheet, without accounting for the effect of the tubes. The values for 600°F were used for the finite element unit load runs. The material properties of the tubes are not utilized in the finite element model, but are listed in Table 7-1 for use in the calculations of the tube/tubesheet contact pressures.

7.1.2 Finite Element Model

The analysis of the contact pressures utilizes conventional (thick shell equations) and finite element analysis techniques. A finite element model was developed for the Model D5-2 SG channel head/tubesheet/shell region (which includes the Byron/Braidwood steam generator) in order to determine the tubesheet rotations. The elements used for the models of the channel head/tubesheet/shell region were the quadratic version of the 2-D axisymmetric isoparametric elements STIF53 and STIF56 of WECAN/Plus (Reference 28). The model for the D5-2 steam generator is shown in Figure 7-2.

The unit loads applied to this model are listed below:

Unit Load	Magnitude
Primary Side Pressure	1000 psi
Secondary Side Pressure	1000 psi
Tubesheet Thermal Expansion	500°F
Shell Thermal Expansion	500°F
Channel Head Thermal Expansion	500°F

The three temperature loadings consist of applying a uniform thermal expansion to each of the three component members, one at a time, while the other two remain at ambient conditions. The boundary conditions imposed for all five cases are: $UX=0$ at all nodes on the centerline, and $UY=0$ at one node on the lower surface of the tubesheet support ring. In addition, an end cap load is applied to the top of the secondary side shell for the secondary side pressure unit load equal to:

$$P_{\text{endcap}} = -\left[\frac{(R_i)^2}{(R_o)^2 - (R_i)^2} \right] P = -9708.43 \text{ psi}$$

where, R_i = Inside radius of secondary shell in finite element model = 64.69 in.
 R_o = Outside radius of secondary shell in finite element model = 67.94 in.
 P = Secondary pressure unit load = 1000 psi.

This yielded displacements throughout the tubesheet for the unit loads.

		a.c.e

The data were fit to the following polynomial equation:

$$[\quad]^{a.c.e}$$

The hole expansion calculation as determined from the finite element results includes the effects of tubesheet rotations and deformations caused by the system pressures and temperatures. It does not include the local effects produced by the interactions between the tube and tubesheet hole. Standard thick shell equations, including accountability for the end cap axial loads in the tube (Reference 29), in combination with the hole expansions from above are used to calculate the contact pressures between the tube and the tubesheet.

The unrestrained radial expansion of the tube OD due to thermal expansion is calculated as:

$$\Delta R_t^{th} = c \alpha_t (T_t - 70)$$

and from pressure acting on the inside and outside of the tube as,

$$\Delta R_{to}^{pr} = \frac{P_i c}{E_t} \left[\frac{(2 - \nu)b^2}{c^2 - b^2} \right] - \frac{P_o c}{E_t} \left[\frac{(1 - 2\nu)c^2 + (1 + \nu)b^2}{c^2 - b^2} \right],$$

- where:
- P_i = Internal primary side pressure, P_{pri} psi
 - P_o = External secondary side pressure, P_{sec} psi
 - b = Inside radius of tube = 0.33943 in.
 - c = Outside radius of tube = 0.382 in.
 - α_t = Coefficient of thermal expansion of tube, in/in/°F
 - E_t = Modulus of Elasticity of tube, psi
 - T_t = Temperature of tube, °F, and,
 - ν = Poisson's Ratio of the material.

The thermal expansion of the hole ID is included in the finite element results and does not have to be expressly considered in the algebra, however, the expansion of the hole ID produced by pressure is given by:

$$\Delta R_{TS}^{pr} = \frac{P_i c}{E_{TS}} \left[\frac{d^2 + c^2}{d^2 - c^2} + \nu \right],$$

where: E_{TS} = Modulus of Elasticity of tubesheet, psi
 d = Outside radius of cylinder which provides the same radial stiffness as the tubesheet, that is, []^{a,c,e}.

If the unrestrained expansion of the tube OD is greater than the expansion of the tubesheet hole, then the tube and the tubesheet are in contact. The inward radial displacement of the outside surface of the tube produced by the contact pressure is given by: (Note: The use of the term δ in this section is unrelated its potential use elsewhere in this report.)

$$\delta_t = \frac{P_2 c}{E_t} \left[\frac{c^2 + b^2}{c^2 - b^2} - \nu \right]$$

The radial displacement of the inside surface of the tubesheet hole produced by the contact pressure between the tube and hole is given by:

$$\delta_{TS} = \frac{P_2 c}{E_{TS}} \left[\frac{d^2 + c^2}{d^2 - c^2} + \nu \right]$$

The equation for the contact pressure P_2 is obtained from:

$$\delta_{t_o} + \delta_{TS} = \Delta R_{t_o} - \Delta R_{TS} - \Delta R_{ROT}$$

where ΔR_{ROT} is the hole expansion produced by tubesheet rotations obtained from finite element results. The ΔR 's are:

$$\Delta R_{t_o} = c \alpha_t (T_t - 70) + \frac{P_{pri} c}{E_t} \left[\frac{(2 - \nu) b^2}{c^2 - b^2} \right] - \frac{P_{sec} c}{E_t} \left[\frac{(1 - 2\nu) c^2 + (1 + \nu) b^2}{c^2 - b^2} \right]$$

$$\Delta R_{TS} = \frac{P_{sec} c}{E_{TS}} \left[\frac{d^2 + c^2}{d^2 - c^2} + \nu \right]$$

The resulting equation is:

$$\left[\right]^{a,c,e}$$

For a given set of primary and secondary side pressures and temperatures, the above equation is solved for selected elevations in the tubesheet to obtain the contact pressures between the tube and tubesheet as a function of radius. The elevations selected ranged from the top to the bottom of the tubesheet. Negative "contact pressure" indicates a gap condition.

The OD of the tubesheet cylinder is equal to that of the cylindrical (simulate) collars (1.80 inches) designed to provide the same radial stiffness as the tubesheet, which was determined from a finite element analysis of a section of the tubesheet (References 30 and 31).

The tube inside and outside radii within the tubesheet are obtained by assuming a nominal diameter for the hole in the tubesheet (0.764 inch) and wall thinning in the tube equal to the average of that measured during hydraulic expansion tests. That thickness is 0.04257 inch for the tube. The following table lists the values used in the equations above, with the material properties evaluated at 600°F. (Note that the properties in the following sections are evaluated at the primary fluid temperature).

Thick Cylinder Equations Parameter	Value
b, inside tube radius, in.	0.33943
c, outside tube radius, in.	0.382
d, outside radius of cylinder w/ same radial stiffness as TS, in.	[] ^{a,c,e}
α_t , coefficient of thermal expansion of tube, in/in °F	$7.83 \cdot 10^{-6}$
E_t , modulus of elasticity of tube, psi	$28.7 \cdot 10^6$
α_{TS} , coefficient of thermal expansion of tubesheet, in/in °F	$7.42 \cdot 10^{-6}$
E_{TS} , modulus of elasticity of tubesheet, psi	$26.4 \cdot 10^6$

7.1.4 Byron/Braidwood 2 Contact Pressures

7.1.4.1 Normal Operating Conditions

The loadings considered in the analysis are based on an umbrella set of conditions as defined in References 26, 27 and 32. The current operating parameters from Reference 33 are used. The temperatures and pressures for normal operating conditions at Byron/Braidwood Unit 2 are bracketed by the following two cases:

Loading	$T_{min}^{(1)}$	$T_{max}^{(2)}$
Primary Pressure	2235 psig	2235 psig
Secondary Pressure	796 psig	938 psig
Primary Fluid Temperature (T_{hot})	608.0°F	620.3°F
Secondary Fluid Temperature	519.8°F	538.8°F
⁽¹⁾ Low T_{ave} with 10% Tube Plugging case in Reference 33 .		
⁽²⁾ High T_{ave} with 0% Tube Plugging case in Reference 33.		

The primary pressure [

]^{a,c,e}.

7.1.4.2 Faulted Conditions

Of the faulted conditions, Feedline Break (FLB) and Steamline Break (SLB) are the most limiting. FLB has a higher ΔP across the tubesheet, while the lower temperature of SLB results in less thermal tightening. Both cases are considered in this section.

Previous analyses have shown that FLB and SLB are the limiting faulted conditions, with tube lengths required to resist push out during a postulated loss of coolant accident (LOCA) typically less than one-fourth of the tube lengths required to resist pull out during FLB and SLB (References 29,30 and 34). Therefore LOCA was not considered in this analysis.

7.1.4.3 Feedline Break

The temperatures and pressures for Feedline Break at Byron/Braidwood Unit 2 are bracketed by the following two cases:

Loading	$T_{min}^{(1)}$	$T_{max}^{(2)}$
Primary Pressure	2835 psig	2835 psig
Secondary Pressure	0 psig	0 psig
Primary Fluid Temperature (T_{hot})	608.0°F	620.3°F
Secondary Fluid Temperature	519.8°F	538.8°F
⁽¹⁾ Low T_{ave} with 10% Tube Plugging case in Reference 33.		
⁽²⁾ High T_{ave} with 0% Tube Plugging case in Reference 33.		

The Feedline Break condition [

j^{a.c.e.}

7.1.4.4 Steam Line Break

As a result of SLB, the faulted SG will rapidly blow down to atmospheric pressure, resulting in a large ΔP across the tubes and tubesheet. The entire flow capacity of the auxiliary feedwater system

would be delivered to the dry, hot shell side of the faulted SG. The primary side re-pressurizes to the pressurizer safety valve set pressure. The hot leg temperature decreases throughout the transient, reaching a minimum temperature of 297°F at 2000 seconds for four loop plants. The pertinent parameters are listed below. The combination of parameters yielding the most limiting results is used.

Primary Pressure	=	2560 psig
Secondary Pressure	=	0 psig
Primary Fluid Temperature (T_{hot})	=	297°F
Secondary Fluid Temperature	=	212°F

For this set of primary and secondary side pressures and temperatures, the equations derived in Section 7.2 below are solved for the selected elevations in the tubesheet to obtain the contact pressures between the tube and tubesheet as a function of tubesheet radius for the hot leg.

7.1.4.5 Summary of FEA Results for Tube-to-Tubesheet Contact Pressures

For Byron/Braidwood 2, the contact pressures between the tube and tubesheet for various plant conditions are listed in Table 7-6 and plotted versus radius in Figure 7-3 through Figure 7-6. The application of these values to the determination of the required engagement length is discussed in Section 7.2.

7.2 Determination of Required Engagement Length of the Tube in the Tubesheet

The elimination of a portion of the tube within the tubesheet from the in-service inspection requirement constitutes a change in the pressure boundary. This is the case regardless of whether or not the inspection is being eliminated in its entirety or if RPC examination is being eliminated when the potential for the existence of circumferential cracks is determined to be necessary for consideration. The elimination of the lower portion of the tube from examination is an H* partial-length RPC justification in the sense of Reference 5 and relies on knowledge of the tube-to-tubesheet interfacial, mechanical interference fit contact pressure at all elevations in the tube joint. In order to maintain consistency with other reports on this subject, the required length of engagement of the tube in the tubesheet to resist performance criteria tube end cap loads is designated by the variable H*. This length is based on structural requirements only and does not include any connotation associated with leak rate, except perhaps in a supporting role with regard to the leak rate expectations relative to normal operating conditions. Since the H* length is usually some distance from the top of the tubesheet, this is especially in the upper half of the tube joint. The contact pressure is used for estimating the magnitude of the anchorage of the tube in the tubesheet over the H* length. It is also used in estimating the impact of changes in the contact pressure on potential primary-to-secondary leak rate during postulated accident conditions.

To take advantage of the tube-to-tubesheet joint anchorage, it is necessary to demonstrate that the [

] ^{a.c.c}

[

] ^{a.c.c}

The end cap loads for Normal and Faulted conditions are:

$$\begin{aligned} \text{Normal (maximum):} & \quad \pi * (2235-796) * (0.764)^2 / 4 = 659.69 \text{ lbs.} \\ \text{Faulted (FLB):} & \quad \pi * 2835 * (0.764)^2 / 4 = 1299.66 \text{ lbs.} \\ \text{Faulted (SLB):} & \quad \pi * 2560 * (0.764)^2 / 4 = 1173.59 \text{ lbs.} \end{aligned}$$

Seismic loads have also been considered, but they are not significant in the tube joint region of the tubes.

A key element in estimating the strength of the tube-to-tubesheet joint during operation or postulated accident conditions is the residual strength of the joint stemming from the expansion preload due to the manufacturing process, i.e., hydraulic expansion. During operation the preload increases because the thermal expansion of the tube is greater than that of the tubesheet and because a portion of the internal pressure in the tube is transmitted to the interface between the tube and the tubesheet. However, the tubesheet bows upward leading to a dilation of the tubesheet holes at the top of the tubesheet and a contraction at the bottom of the tubesheet when the primary-to-secondary pressure difference is positive. The dilation of the holes acts to reduce the contact pressure between the tubes and the tubesheet. The H* lengths are based on the pullout resistance associated with the net contact pressure during normal or accident conditions. The calculation of the residual strength involves a conservative approximation that the strength is uniformly distributed along the entire length of the tube. This leads to a lower bound estimate of the strength and relegates the contribution of the preload to having a second order effect on the determination of H*.

A series of tests were performed to determine the residual strength of the joint. The data from this series of pullout tests are listed in Table 7-12. Three (3) each of the tests were performed at room

temperature, 400°F, and 600°F. (Note: Three other tests were performed with internal pressure in the tube. However, in these tests, the resistance to pullout was so great that the tube yielded, furnishing only input information of joint lower bound strength. These data were not used.) [

J^{a.c.e}

The force resisting pullout acting on a length of a tube between elevations h_1 and h_2 is given by:

$$F_i = (h_2 - h_1)F_{HE} + \mu\pi d \int_{h_1}^{h_2} Pdh$$

where: F_{HE} = Resistance to pull out due to the initial hydraulic expansion = 326.8 lb/inch,
 P = Contact pressure acting over the incremental length segment dh , and,
 μ = Coefficient of friction between the tube and tubesheet, conservatively assumed to be 0.2 for the pullout analysis to determine H^* .

The contact pressure is assumed to vary linearly between adjacent elevations in the top part of Table 7-7 through Table 7-11, so that between elevations L_1 and L_2 ,

$$P = P_1 + \frac{(P_2 - P_1)}{(L_2 - L_1)}(h - L_1)$$

or,

$$\left[\dots \right]^{a.c.e}$$

so that,

$$\left[\dots \right]^{a.c.e}$$

This equation was used to accumulate the force resisting pullout from the top of the tubesheet to each of the elevations listed in the lower parts of Table 7-7 through Table 7-11. The above equation is also used to find the minimum contact lengths needed to meet the pullout force requirements. In Zone C, the length calculated was 7.03 inches for the 3 times the normal operating pressure performance criterion which corresponds to a pullout force of 1979 lbf in the Hot Leg.

The top part of Table 7-9 lists the contact pressures through the thickness at each of the radial sections for Faulted (SLB) condition. The last row, "h(0)," of this part of the table lists the maximum tubesheet elevation at which the contact pressure is greater than or equal to zero. The above equation is used to accumulate the force resisting pull out from the top of the tubesheet to each of the elevations listed in the lower part of Table 7-9. In Zone C, this length is 8.61 inches for the 1.43 times the accident pressure performance criterion which corresponds to a pullout force of 1859 lbs in the Hot Leg for the Faulted (SLB) condition. The minimum contact length needed to meet the pullout force requirement of 1859 lb. for the Faulted (FLB) condition is less as is shown in Table 7-10 and Table 7-11. The H* calculations for each loading condition at each of the radii considered are summarized in Table 7-13. The H* results for each zone are summarized in Table 7-14.

Therefore, the bounding condition for the determination of the H* length is the SLB performance criterion. The minimum contact length for the SLB faulted condition is 8.61 inches in Zone C, Reference 35.

In Zone B, The SLB performance criterion is controlling and the minimum contact length is 5.99 inches. In Zone A, however, the normal operating condition is controlling and the minimum contact length is calculated to be 2.65 inches.

Table 7-1. Summary of Material Properties Alloy 600 Tube Material

Property	Temperature (°F)						
	70	200	300	400	500	600	700
Young's Modulus (psi·10 ⁶)	31.00	30.20	29.90	29.50	29.00	28.70	28.20
Thermal Expansion (in/in·°F·10 ⁻⁶)	6.90	7.20	7.40	7.57	7.70	7.82	7.94
Density (lb-sec ² /in ⁴ ·10 ⁻⁴)	7.94	7.92	7.90	7.89	7.87	7.85	7.83
Thermal Conductivity (Btu/sec-in·°F·10 ⁻⁴)	2.01	2.11	2.22	2.34	2.45	2.57	2.68
Specific Heat (Btu-in/lb-sec ² -°F)	41.2	42.6	43.9	44.9	45.6	47.0	47.9

Table 7-2. Summary of Material Properties for SA-508 Class 2a Tubesheet Material

Property	Temperature (°F)						
	70	200	300	400	500	600	700
Young's Modulus (psi·10 ⁶)	29.20	28.50	28.00	27.40	27.00	26.40	25.30
Thermal Expansion (in/in·°F·10 ⁻⁶)	6.50	6.67	6.87	7.07	7.25	7.42	7.59
Density (lb-sec ² /in ⁴ ·10 ⁻⁴)	7.32	7.30	7.29	7.27	7.26	7.24	7.22
Thermal Conductivity (Btu/sec-in·°F·10 ⁻⁴)	5.49	5.56	5.53	5.46	5.35	5.19	5.02
Specific Heat (Btu-in/lb-sec ² -°F)	41.9	44.5	46.8	48.8	50.8	52.8	55.1

Table 7-3. Summary of Material Properties SA-533 Grade A Class 2 Shell Material

Property	Temperature (°F)						
	70	200	300	400	500	600	700
Young's Modulus (psi·10 ⁶)	29.20	28.50	28.00	27.40	27.00	26.40	25.30
Thermal Expansion (in/in·°F·10 ⁻⁶)	7.06	7.25	7.43	7.58	7.70	7.83	7.94
Density (lb-sec ² /in ⁴ ·10 ⁻⁴)	7.32	7.30	7.283	7.265	7.248	7.23	7.211

Table 7-4. Summary of Material Properties SA-216 Grade WCC Channelhead Material

Property	Temperature (°F)						
	70	200	300	400	500	600	700
Young's Modulus (psi·10 ⁶)	29.50	28.80	28.30	27.70	27.30	26.70	25.50
Thermal Expansion (in/in/°F·10 ⁻⁶)	5.53	5.89	6.26	6.61	6.91	7.17	7.41
Density (lb-sec ² /in ⁴ ·10 ⁻⁴)	7.32	7.30	7.29	7.27	7.26	7.24	7.22

**Table 7-5. Equivalent Solid Plate Elasticity Coefficients for D5 Perforated TS
SA-508 Class 2a Tubesheet Material**

a,c,e

Table 7-9. Cumulative Forces Resisting Pull Out from the TTS Byron/Braidwood 2-Faulted (SLB) Conditions

a,c,e

Table 7-14. H* Summary Table

Zone	Limiting Loading Condition	Engagement from TTS (inches)
A	3.0 NO ΔP ^(1,2)	2.95 ⁽³⁾
B	1.43 SLB ΔP ^(1,2)	6.00
C	1.43 SLB ΔP ^(1,2)	8.61
<p>Notes:</p> <ol style="list-style-type: none"> 1. Seismic loads have been considered and are not significant in the tube joint region (Reference 37). 2. The scenario of tubes locked at support plates is not considered to be a credible event in Model D5 SGs as they are manufactured with stainless steel support plates. However, conservatively assuming that the tubes become locked at 100% power conditions, the maximum force induced in an active tube as the SG cools to room temperature is []^{a.c.e} 3. 0.3 inches added to the maximum calculated H* for Zone A to account for the hydraulic expansion transition region at the top of the tubesheet. 		

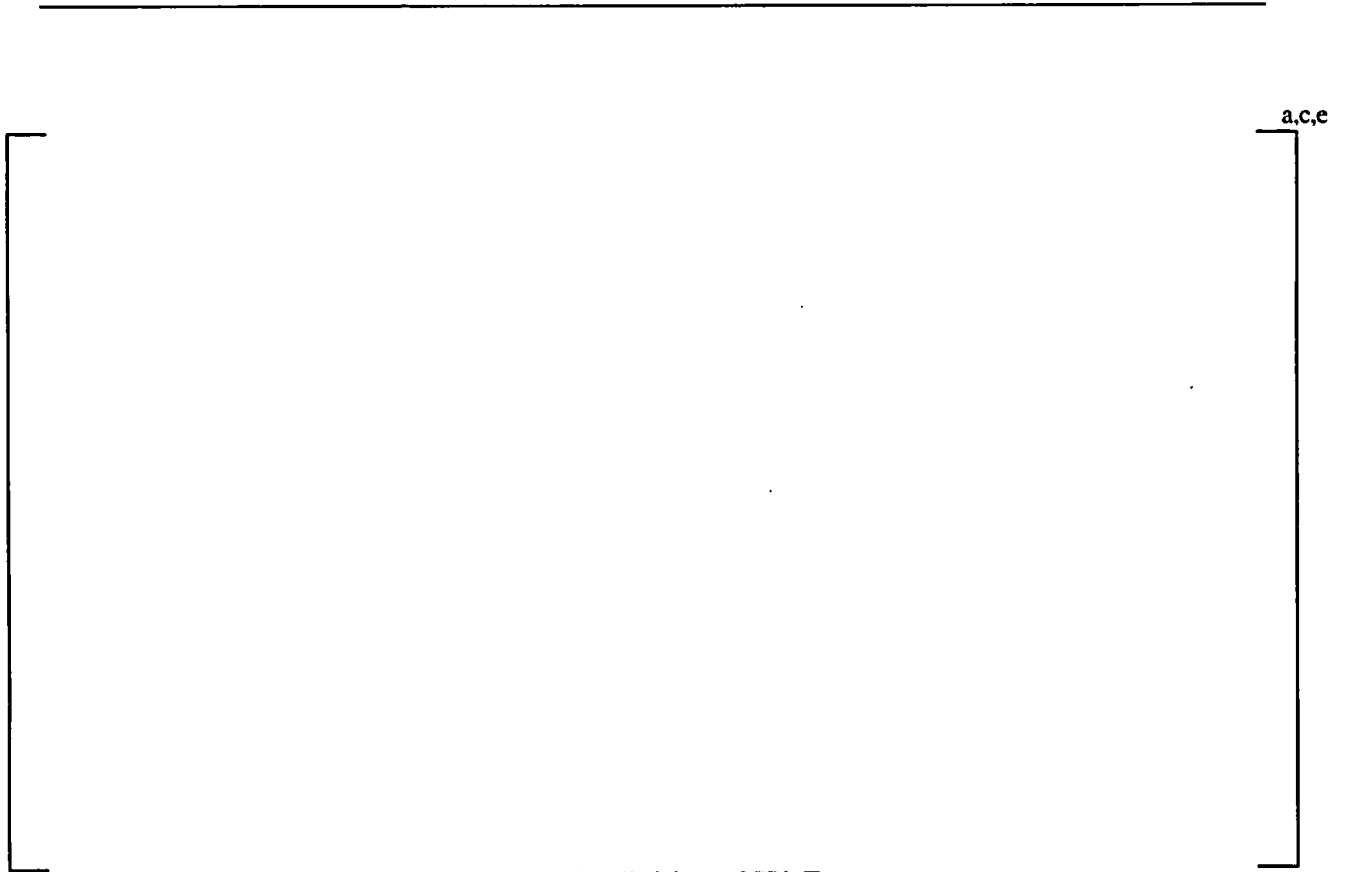


Figure 7-1. Definition of H* Zones

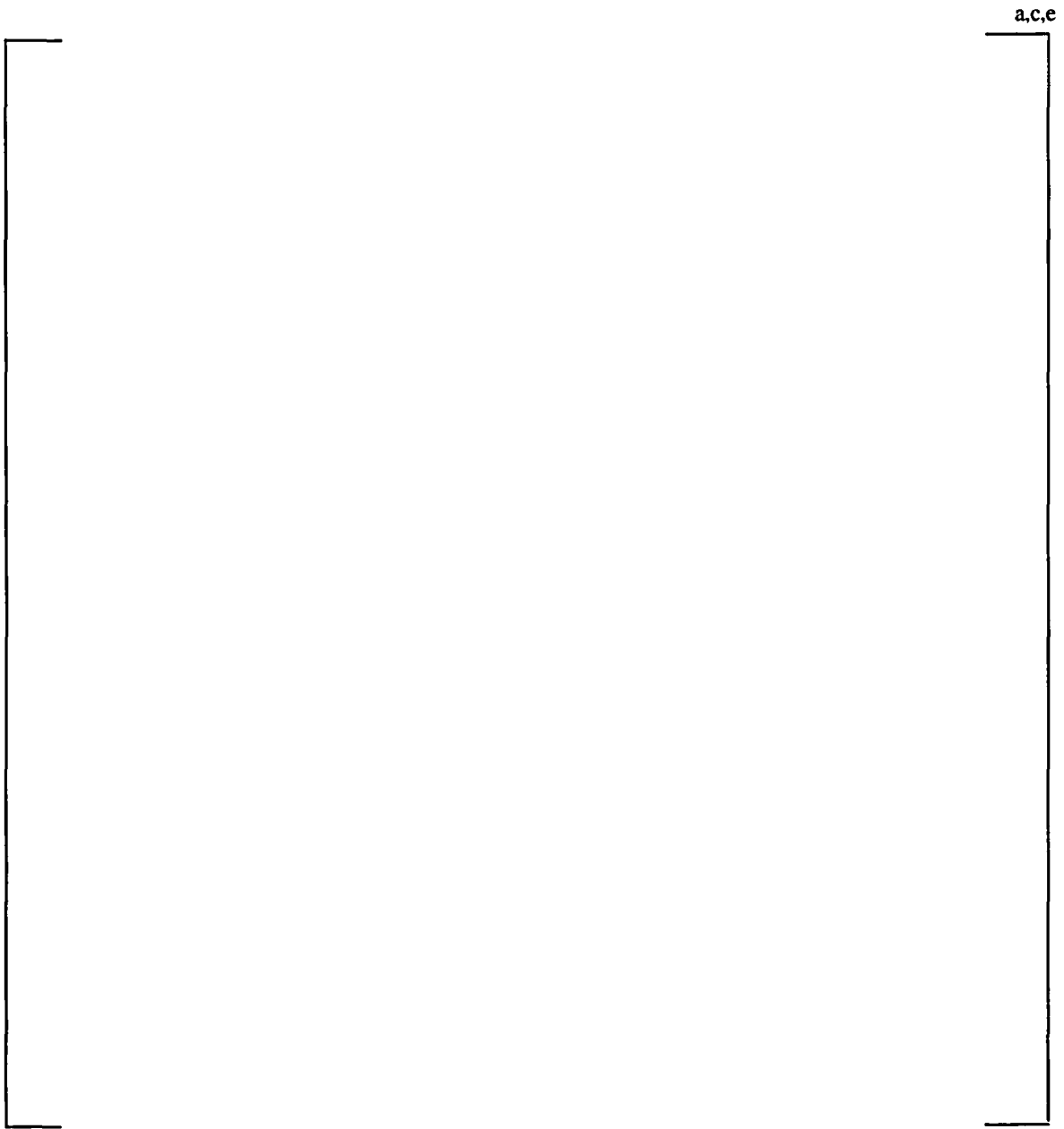


Figure 7-2. Finite Element Model of Model D5-3 Tubesheet Region

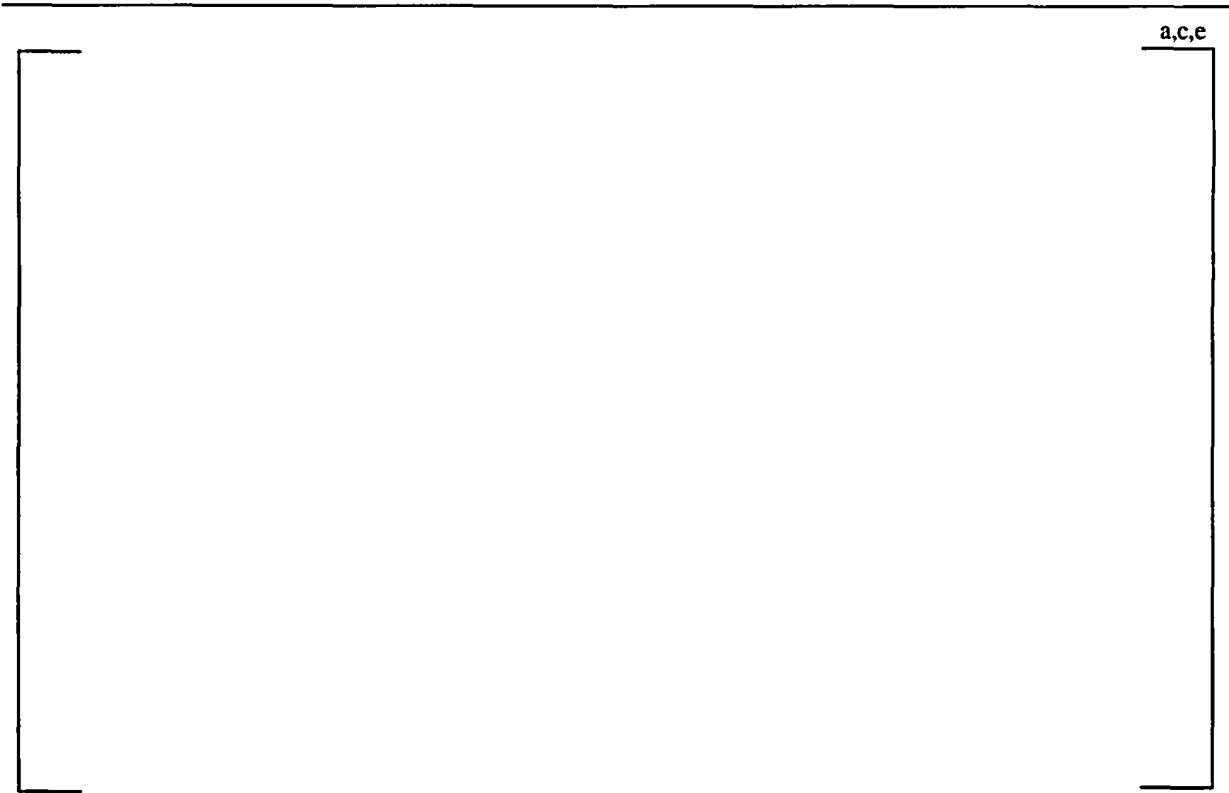


Figure 7-3. Contact Pressures for Normal Condition (T_{min}) at Byron/Braidwood 2



Figure 7-4. Contact Pressures for Normal Condition (T_{max}) at Byron and Braidwood Unit 2

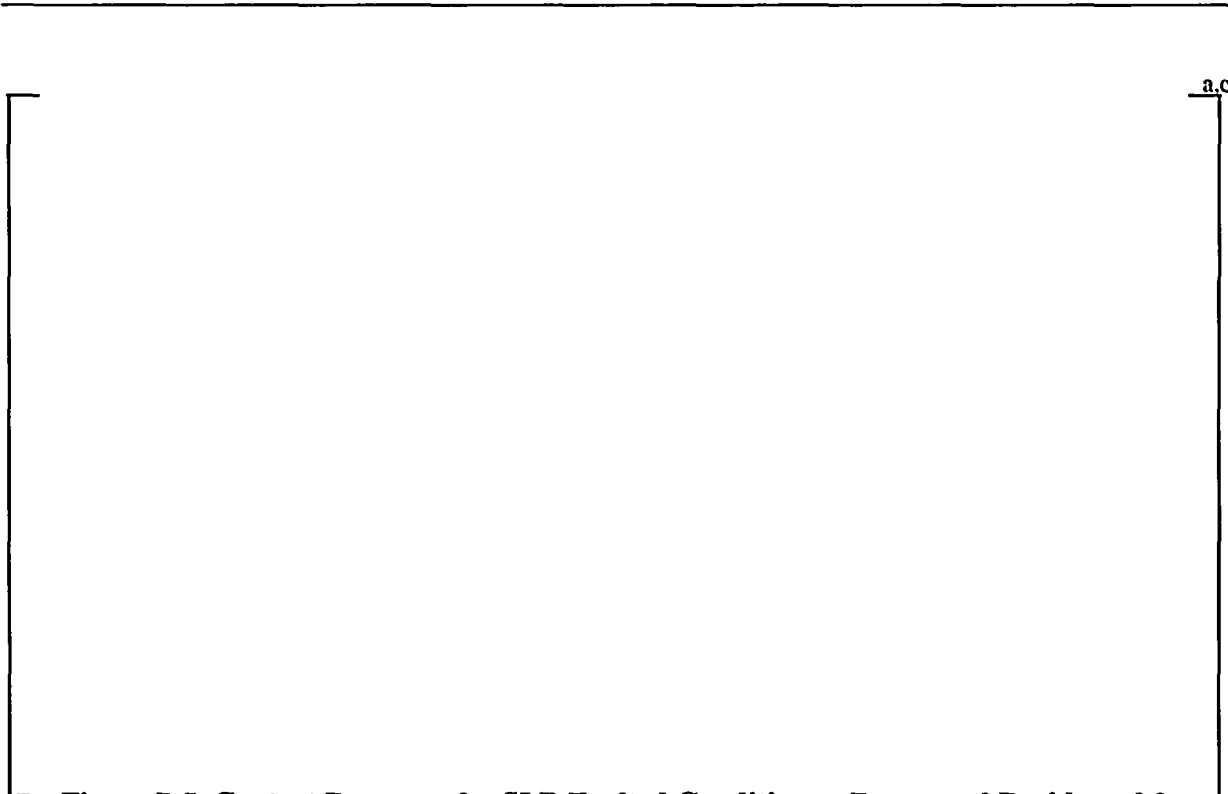


Figure 7-5. Contact Pressures for SLB Faulted Condition at Byron and Braidwood 2



Figure 7-6. Contact Pressures for FLB Faulted Condition at Byron and Braidwood 2 (Tmin)

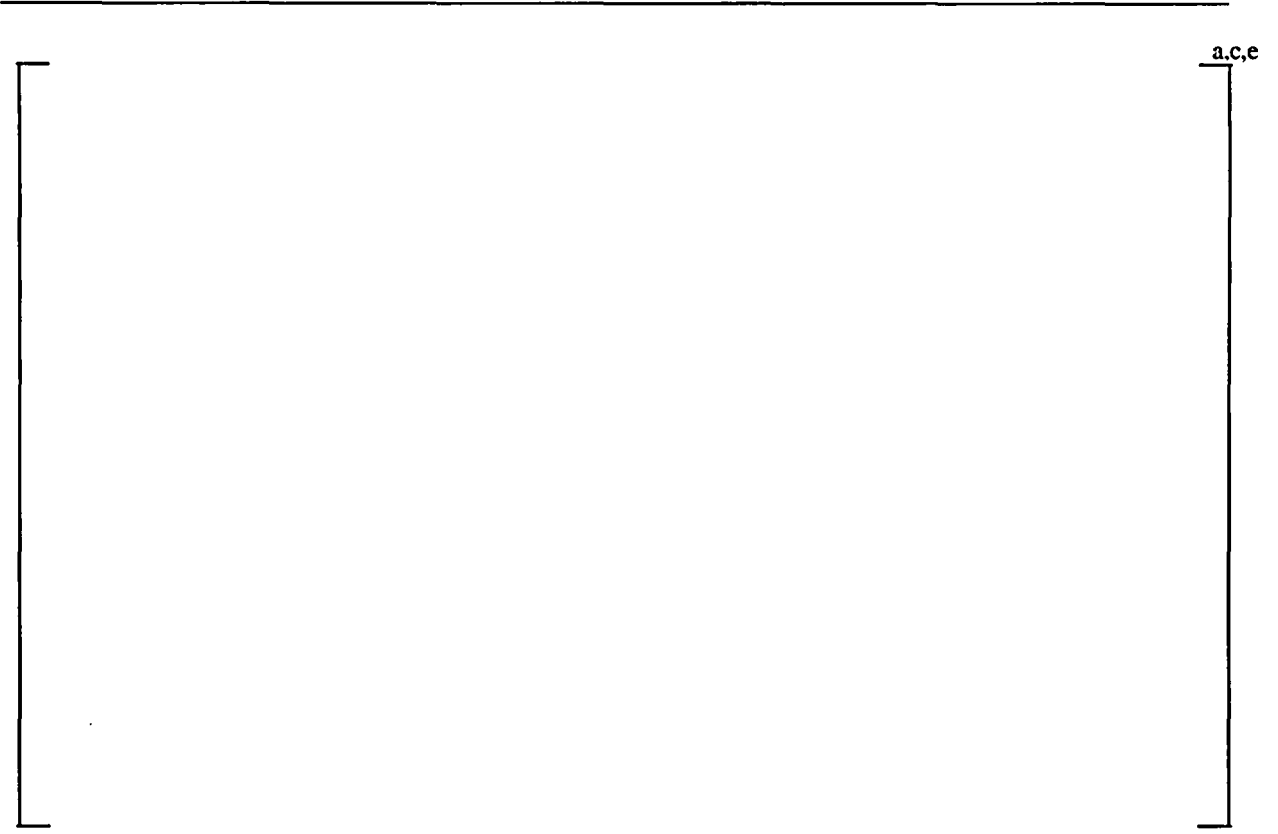


Figure 7-7. Contact Pressures for FLB Faulted Condition at Byron and Braidwood 2 (Tmax)



Figure 7-8. D5 Pullout Test Results for Force/inch at 0.25 inch Displacement

8.0 Leak Rate Analysis of Cracked Tube-to-Tubesheet Joints

This section of the report presents a discussion of the leak rate expectations from axial and circumferential cracking confined to the tube-to-tubesheet joint region, including the tack expansion region, the tube-to-tubesheet welds and areas where degradation could potentially occur due to bulges and overexpansions within the tube at a distance at or below 17 inches from the top of the tubesheet. Although the welds are not part of the tube per the technical specifications, consideration is given in deference to the discussions of the NRC staff in References 2 and 8. It is noted that the methods discussed below support a permanent change to the Byron 2/Braidwood 2 Technical Specification. The approval for the change to the Braidwood 2 Technical Specification on a one cycle bases was obtained in April 2005. With regard to the inherent conservatism embodied in the application of any predictive methods it is noted that the presence of cracking was not confirmed because removal of a tube section was not performed at Catawba 2 or Vogtle 1.

8.1 The Bellwether Principle for Normal Operation to Steam Line Break Leak Rates

From an engineering expectation standpoint, if there is no meaningful primary-to-secondary leakage during normal operation, there should likewise be no meaningful leakage during postulated accident conditions from indications located below the mid-plane of the tubesheet. The rationale for this is based on considerations regarding the deflection of the tubesheet with accompanying dilation and diminution of the tubesheet holes. In effect, the area presented as a leak path between the tube and tubesheet would not be expected to increase under postulated accident conditions and would really be expected to decrease for most of the SG tubes. During the development of the H* criteria, consideration was given of the potential for leak rate during normal operation to act as a bellwether or leading indicator with regard to the leak rate that could be expected during postulated accident conditions. The results from these considerations were not included in the final versions of the H* document because of concerns associated with the accuracy of the approach for indications above the neutral plane of the tubesheet where the tube-to-tubesheet contact pressure would usually be expected to diminish during faulted conditions. For example, if it was intended to stop the RPC examination at a depth of 3 to 9 inches from the top of the tubesheet, then severe circumferential cracking would have been postulated to occur immediately below that depth and the potential leak rate as compared to that during normal operation estimated. The primary-to-secondary pressure difference during normal operation is on the order of 1200 to 1400 psi, while that during a postulated accident, e.g., steam line and feed line break, is on the order of 2560 to 2650 psi.³ Above the neutral plane of the tubesheet the tube holes experience a dilation due to pressure induced bow of the tubesheet. This means that the contact pressure between the tubes and the tubesheet would diminish above the neutral plane in the central region of the tubesheet at the same time as the driving potential would increase, leading to an expectation of an increase in the potential leak rate through the crevice. Estimating the change in leak rate as a function of the change in contact pressure under faulted conditions on a generic basis was expected to be problematic. However, below the neutral plane of the tubesheet the tube holes diminish in size because of the

upward bending and the contact pressure between the tube and the tubesheet increases. When the differential pressure increases during a postulated faulted event the increased bow of the tubesheet leads to an increase in the tube-to-tubesheet contact pressure, increasing the resistance to flow. Thus, while the dilation of the tube holes above the neutral plane of the tubesheet presents additional analytic problems in estimating the leak rate for indications above the neutral plane, the diminution of the holes below the neutral plane presents definitive statements to be made with regard to the trend of the leak rate, hence, the bellwether principle. Independent consideration of the effect of the tube-to-tubesheet contact pressure leads to similar conclusions with regard to the opening area of the cracks in the tubes, thus further restricting the leak rate beyond that through the interface between the tube and the tubesheet.

In order to accept the concept of normal operation being a bellwether for the postulated accident leak rate for indications above the neutral plane of the tubesheet, the change in leak rate had to be quantified using a somewhat complex, physically sound model of the thermal-hydraulics of the leak rate phenomenon. This is not necessarily the case for cracks considered to be present below the neutral plane of the tubesheet. This is because a diminution of the holes takes place during postulated accident conditions below the neutral plane relative to normal operation. For example, at a radius of approximately 34 inches from the center of the SG, the contact pressure during normal operation is calculated to be about 2010 to 2200 psi³, see the last contact pressure entry in the center columns of Table 7-8 and Table 7-7 respectively, while the contact pressure during a postulated steam line break would be on the order of 3320 psi at the bottom of the tubesheet, Table 7-9, and during a postulated feed line break would be on the order of 4250 to 4290 psi at the bottom of the tubesheet, Table 7-10 and Table 7-11 respectively. (Note: The radii specified in the heading of the tables are the maximum values for the respective zones analyzed, hence the contact pressures in the center column correspond to the radius specified for the left column, etc. The leftmost column lists the contact pressure values for a radius of 4.08 inches.) The analytical model for the flow through the crevice, the Darcy equation for flow through porous media, indicates that flow would be expected to be proportional to the differential pressure. Thus, a doubling of the leak rate could be predicted if the change in contact pressure between the tube and the tubesheet were ignored. Examination of the nominal correlation on Figure 6-6 indicates that the resistance to flow (the loss coefficient) would increase by a factor of about 3 during a postulated SLB event.

The leak rate from a crack located within the tubesheet is governed by the crack opening area, the resistance to flow through the crack, and the resistance to flow provided by the tube-to-tubesheet joint. The path through the tube-to-tubesheet joint is also frequently referred to as a crevice, but is not to be confused with the crevice left at the top of the tubesheet from the expansion process. The presence of the joint makes the flow from cracks within the tubesheet much different from the flow to be expected from cracks outside of the tubesheet. The tubesheet prevents outward deflection of the flanks of cracks, a more significant effect for axial than for circumferential cracks, which is a significant contributor to the opening area presented to the flow. In addition, the restriction

³ The differential pressure may be on the order of 2405 psi if it is demonstrated that the power operated relief valves will be functional.

⁴ The change occurs as a result of considering various hot and cold leg operating temperatures.

provided by the tubesheet greatly restrains crack opening in the direction perpendicular to the flanks regardless of the orientation of the cracks. The net effect is a large, almost complete reduction of the leak rate when the tube cracks are within the tubesheet.

The leak path through the crack and the crevice is very tortuous. The flow must go through many turns within the crack in order to pass through the tube wall, even though the tube wall thickness is relatively small. The flow within the crevice must constantly change direction in order to follow a path that is formed between the points of hard contact between the tube and the tubesheet as a result of the differential thermal expansion and the internal pressure in the tube. There is both mechanical dispersion and molecular diffusion taking place. The net result is that the flow is best described as primary-to-secondary weepage. At its base, the expression used to predict the leak rate from tube cracks through the tube-to-tubesheet crevice is the Darcy expression for flow rate, Q , through porous media, i.e.,

$$Q = \frac{1}{K\mu} \frac{dP}{dz}, \quad (1)$$

where μ is the viscosity of the fluid, P is the driving pressure, z is the physical dimension in the direction of the flow, and K is the “loss coefficient” which can also be termed the flow resistance if the other terms are taken together as the driving potential. The loss coefficient is found from a series of experimental tests involving the geometry of the particular tube-to-tubesheet crevice being analyzed, including factors such as surface finish, and then applied to the cracked tube situation.

If the leak rate during normal operation was 0.104 gpm (150 gpd), the postulated accident condition leak rate would be on the order of 0.2 gpm considering only the change in differential pressure, but the estimate would be reduced to 0.07 gpm (based on a factor of 3 increase in flow resistance) when the increase in contact pressure is included during a postulated steam line break event, i.e., about 70% of that during normal operation. This latter value is significantly less than the allowable limit during faulted conditions of 0.5 gpm at room temperature density. Even without inclusion of the effect of the change in contact pressure, the predicted leak rate would be significantly less than the allowable rate of 0.5 gpm.

The above argument considered indications located where the expectations associated with the bellwether principle would be a maximum, i.e., where the relative increase in contact pressure from normal to faulted conditions is a maximum. Thus, the conclusions of this section apply directly to indications in the tube somewhat near the bottom of the tubesheet, i.e., as a minimum to tube indications within a little more than 4 inches from the bottom of the tubesheet and to postulated indications in the tube-to-tubesheet welds. An examination of the contact pressures as a function of depth in the tubesheet from the finite element analyses of the tubesheet as reported in Table 7-7 through Table 7-11 shows that the bellwether principle applies to a significant extent to all indications below the neutral plane of the tubesheet. At the central plane of the tubesheet the increase in contact pressure is more on the order of 15% relative to that during normal operation for all tubes regardless of radius. Still, the fact that the contact pressure increases means that the leak rate would be expected to be bounded by a factor of two relative to normal operation. At a

depth of 17 inches from the top of the tubesheet the contact pressure increases by about 50% relative to that during normal operation. The flow resistance would be expected to increase by about 60%, thus the increase in driving pressure would be mostly offset by the increase in the resistance of the joint.

The numerical results from the finite element analyses are presented on Figure 8-1 at the elevation of the mid-plane of the tubesheet through Figure 8-4 at the bottom of the tubesheet. A comparison of the contact pressure during postulated SLB conditions relative to that during normal operation is provided for depths of 10.5, 12.6, 16.9, and 21 inches below the top of the tubesheet, the last being at the bottom of the tubesheet.

- At roughly the neutral surface, about 10.5 inches, the contact pressure during SLB is uniformly greater than that during normal operation by about 270 psi (ranging from 255 to 291 psi).
- At a depth of 12.6 inches the contact pressure increase ranges from a maximum of 537 psi near the center of the tubesheet to 275 psi at a radius of 55 inches, see Figure 8-2.
- At 16.9 inches below the top of the tubesheet and 4.13 inches above the bottom of the tubesheet the contact pressure increases by a maximum of 821 psi to a minimum of 236 psi at a radius of 56 inches, Figure 8-3.
- At the bottom of the tubesheet, Figure 8-4, the contact pressure increases by over 1700 psi near the center of the tubesheet, exhibits no change at a radius of about 55 inches, and diminishes by 369 psi at the extreme periphery, a little less than 61 inches from the center.

At a depth of about 6 inches from the top of the tubesheet the contact pressure decreases by about 370 psi near the center of the tubesheet, is unchanged at a radius of about 42 inches and increases by a maximum of 251 psi at a radius of 58 inches. A similar comparison is illustrated on Figure 8-5 at a depth of 8.25 inches from the top of the tubesheet, roughly equal to the originally derived H^* depth for the worst location in the tubesheet as determined using SLB conditions. Here the contact pressure decreases at most by 53 psi at a radius of 3.1 inches, is unchanged at a radius of 21 inches, and increases by a maximum of 268 psi at a radius of 56.9 inches. The density of the number of tubes populating the tubesheet increases with the square of the radius, thus, even at the H^* depth there are far more tubes for which the contact pressure is unchanged or increases at that elevation than there are tubes for which the contact pressure decreases, i.e., 88% of the tubes are at a radius greater than 21 inches from the center of the tubesheet.

The leak rate from any indication is determined by the total resistance of the crevice from the elevation of the indication to the top of the tubesheet, ignoring the resistance from the crack itself. Thus, it would not be sufficient to simply use the depth of 8.25 inches and suppose that the leak rate would be relatively unchanged even if the pressure potential difference were the same. However, the fact that the contact pressure generally increases below that elevation indicates that the leak rate would be relatively unaffected for indications a little deeper into the tubesheet. For example, it would be expected that the leak rate would not increase meaningfully from any indications below the mid-plane of the tubesheet. A comparison of the curves on Figure 8-5 relative

to those on Figure 7 indicates that the contact pressure generally increases for a length of at least 2 inches upward from the mid-plane for tubes with a radius of 21 inches from the center of the tubesheet. For radial locations greater than 21 inches from the center of the tubesheet the length for which the contact pressure increases would be greater than 2 inches.

The trend is consistent, at radii where the contact pressure decreases or the increase is not as great near the bottom of the tubesheet, the increase at higher elevations would be expected to compensate. For example, the contact pressures on Figure 8-4 at the bottom of the tubesheet show a decrease beyond a radius of 55 inches, however, the increase at 8.4 inches above the bottom, Figure 8-2 is significant. For the outboard tubes the increase in contact pressure extends all the way to the top of the tubesheet.

A comparison of the curves at the various elevations leads to the conclusion that for a length of 8 inches upward from an elevation of 4.23 inches above the bottom of the tubesheet there is always an increase in the contact pressure in going from normal operation conditions to postulated SLB conditions. Hence, it is reasonable to omit any consideration of inspection of bulges or other artifacts below a depth of 17 inches from the top of the tubesheet. Therefore, applying a very conservative inspection sampling length of 17 inches downward from the top of the tubesheet during the Braidwood 2 and the Byron 2 outages provides a high level of confidence that the potential leak rate from indications below the lower bound inspection elevation during a postulated SLB event will be bounded by twice the normal operation primary-to-secondary leak rate.

8.2 Ligament Tearing Discussion

One of the concerns that must be addressed in dealing with cracks in SG tubes is the potential for ligament tearing to occur during a postulated accident when the differential pressure is significantly greater than during normal operation. While this is accounted for in the strength evaluations that demonstrate a resistance to pullout in excess of $3 \cdot \Delta P$ for normal operation and $1.4 \cdot \Delta P$ for postulated accident conditions, the potential for ligament tearing to significantly affect the leak rate predictions needs to be accounted for.

Ligament tearing considerations for circumferential tube cracks that are located below the H^* depths within the tubesheet are significantly different from those for potential cracks at other locations. The reason for this is that H^* has been determined using a factor of safety of three relative to the normal operating pressure differential and 1.4 relative to the most severe accident condition pressure differential. Therefore, the internal pressure end cap loads which normally lead to an axial stress in the tube are not transmitted below about $2/3$ of the H^* depth. This means that the only source of stress acting to extend the crack is the primary pressure acting on the flanks of the crack. Since the tube is captured within the tubesheet, there are additional forces acting to resist opening of the crack. The contact pressure between the tube and tubesheet results in a friction induced shear stress acting opposite to the direction of crack opening, and the pressure on the flanks is compressive on the material adjacent to the plane of the crack, hence a Poisson's ratio radial expansion of the tube material in the immediate vicinity of the crack plane is induced which also acts to restrain the opening of the crack. In addition, the differential thermal expansion of the

tube is greater than that of the carbon steel tubesheet, thereby inducing a compressive stress in the tube below the H* length.

A scoping evaluation of the [

]a.c.e.

In summary, considering the worst-case scenario, the likelihood of ligament tearing from radial circumferential cracks resulting from an accident pressure increase is small since at most, only 9% of the cross-sectional area is needed to maintain tube integrity. Also, since the crack face area will be less than the total cross-sectional area used above, the difference in the force applied as a result of normal operating and accident condition pressures will be less than the 58 lbs associated with the above numbers. Therefore, the potential for ligament tearing is considered to be a secondary effect of essentially negligible probability and should not affect the results and conclusions reported for the H* evaluation. The leak rate model does not include provisions for predicting ligament tearing and subsequent leakage, and increasing the complexity of the model to attempt to account for ligament tearing has been demonstrated to be not necessary (Reference 38).

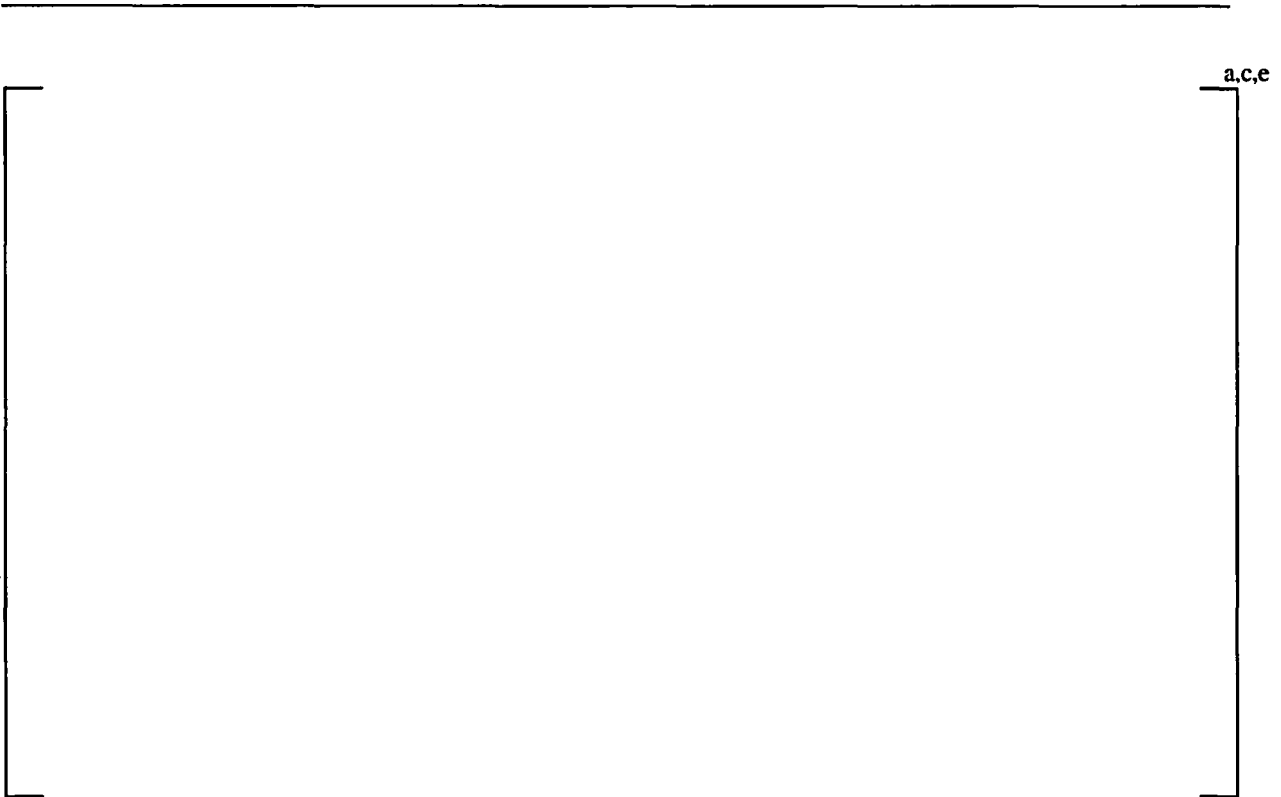


Figure 8-1. Change in contact pressure at 10.5 inches below the TTS



Figure 8-2. Change in contact pressure at 12.6 inches below the TTS

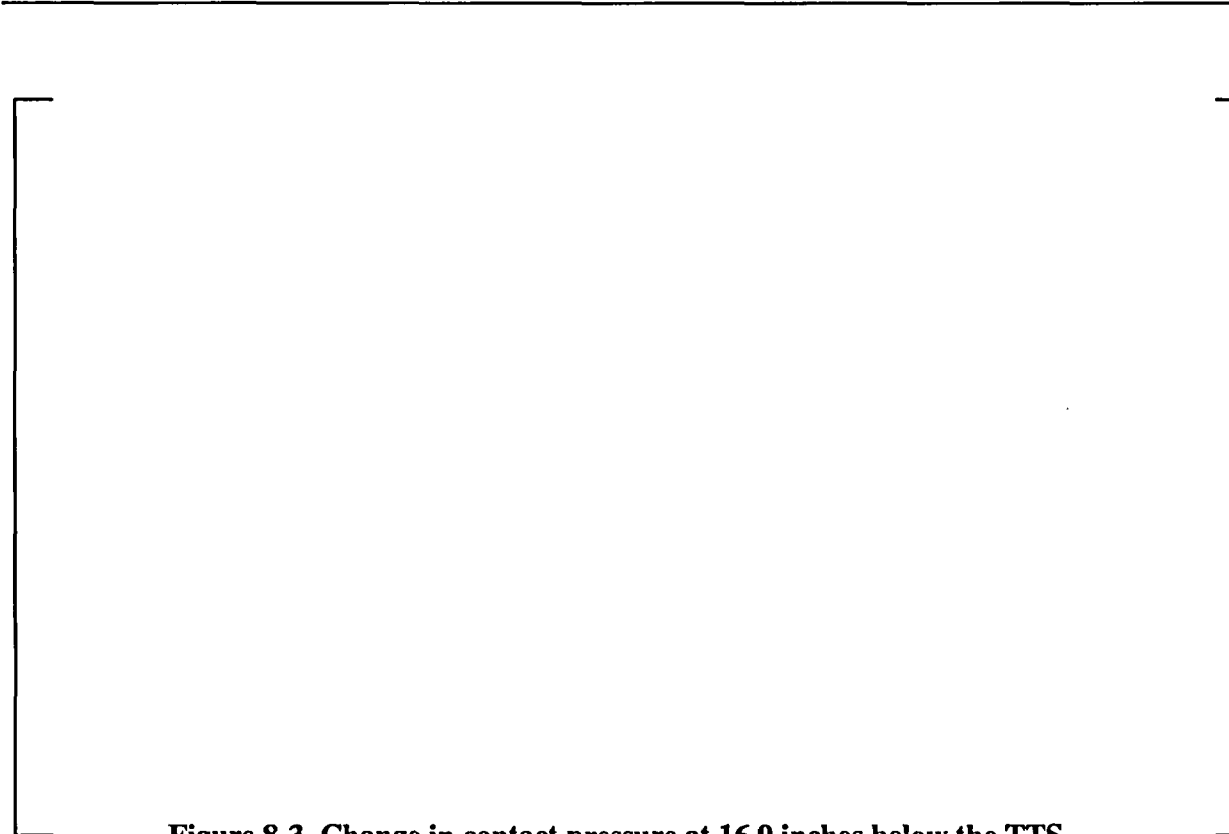


Figure 8-3. Change in contact pressure at 16.9 inches below the TTS



Figure 8-4. Change in contact pressure at the bottom of the tubesheet

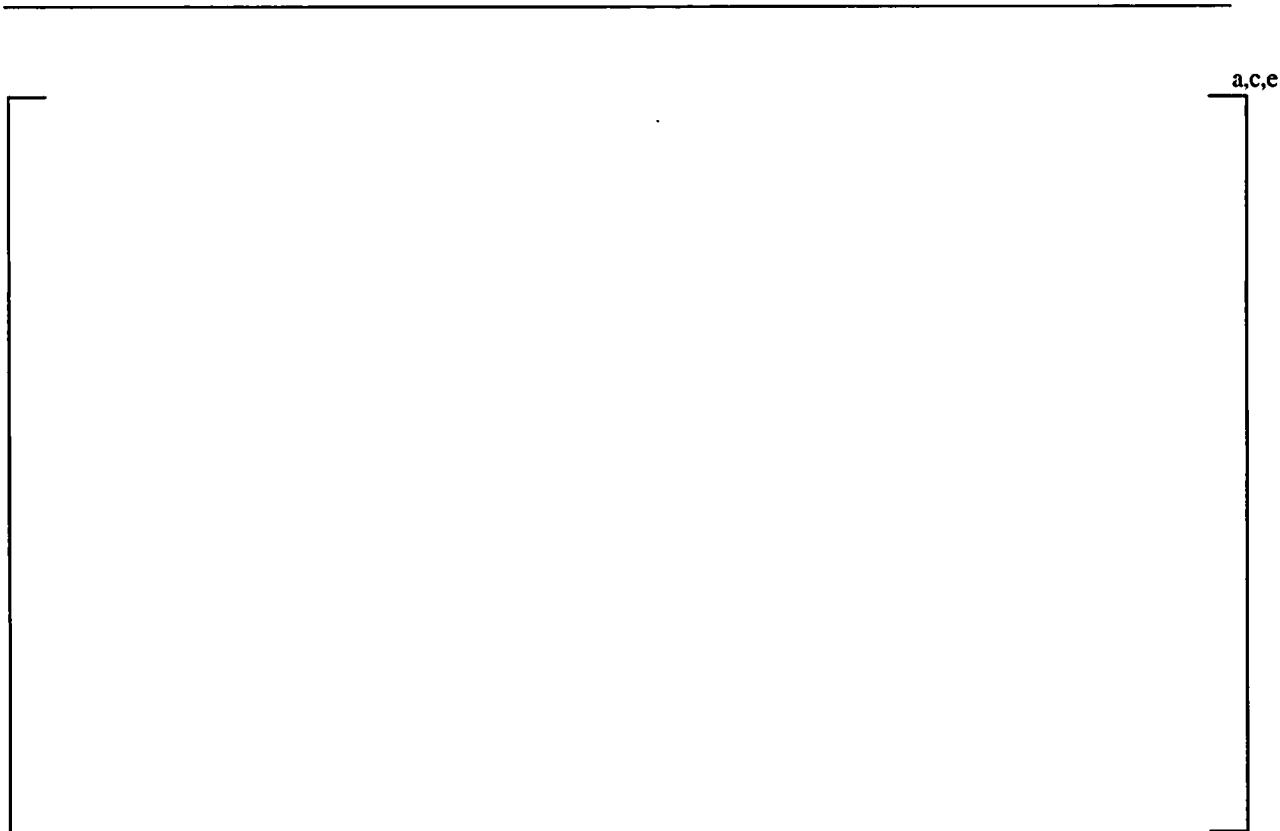


Figure 8-5. Change in contact pressure at 8.25 inches below the TTS

9.0 Review of Qualitative Arguments Used by the NRC Staff for One Cycle Approval of the Tube Joint Eddy Current Inspection Length for Braidwood Unit 2

9.1 Joint Structural Integrity Discussion

As noted in Section 4.1, "Joint Structural Integrity" of Reference 9, the NRC stated that the Westinghouse analyses that concluded that the required engagement distances that varies from 3 to 8.6 inches were not reviewed in detail and more qualitative arguments are used by the NRC staff for one time approval of the 17 inch tube joint inspection length. The qualitative arguments are stated below.

Pullout tests demonstrate that the radial contact pressure produced by the hydraulic expansion alone is such as to require an engagement distance of 6 inches to ensure adequate safety margins against pullout. This estimate is a mean minus one standard deviation based on nine pullout tests. The estimate ignores that effect on needed engagement distance from differential thermal expansion, and tubesheet bore dilations associated with tubesheet bow.

Radial differential thermal expansion between the tube and the tubesheet under hot operating conditions will act to further tighten the joint (i.e., increase radial contact pressure) and to reduce the necessary engagement distance relative to room temperature conditions. The radial differential thermal expansion arises from the fact that Alloy 600 tubing has a slightly higher (by 6 percent) coefficient of thermal expansion than does the SA-508 Class 2a tubesheet material and that tubes are a little hotter than the tubesheet.

The internal primary pressure inside the tube under normal operating and accident conditions also acts to tighten the joint relative to unpressurized conditions, thus reducing the necessary engagement distance.

Tubesheet bore dilations caused by the tubesheet bow under primary to secondary pressure can increase or decrease contact pressure depending on tube location within the bundle and the location along the length of the tube in the tubesheet region. Basically, the tubesheet acts as a flat, circular plate under an upward acting net pressure load. The tubesheet is supported axially around its periphery with a partial restraint against tubesheet rotation provided by the steam generator shell and the channel head. The SG divider plate provides a spring support against upward displacement along a diametral mid-line. Over most of the tubesheet away from the periphery, the bending moment from the resulting from the applied primary to secondary pressure load can be expected to put the tubesheet in tension at the top and compression at the bottom. Thus, the resulting distortion of the tubesheet bore (tubesheet bore dilation) tends to be such as to loosen the tube to tubesheet joint at the top of the tubesheet and to tighten the joint at the bottom of the tubesheet. The amount of dilation and resulting change in joint contact pressure would be expected to vary in a linear fashion from the top to the bottom of a tubesheet. Given the neutral axial to be at approximately the mid-point of the tubesheet thickness (i.e., 10.5 inches below the TTS to 17 inches below the TTS), tubesheet bore dilation effects would be expected to further tighten the joint from 10 inches below the TTS to 17 inches below the TTS which would be the lower limit of the proposed tubesheet region inspection zone. Combined with the effects of the tube joint

tightening associated with the radial differential thermal expansion and primary pressure inside the tube, contact pressure over at least a 6.5 inch distance should be considerably higher than the contact pressure simulated in the above mentioned pullout tests. A similar logic applied to the periphery of the tubesheet leads the staff to conclude that at the top 10.5 inches of the tubesheet region, contact pressure over at least a 6.5 inch distance should be considerably higher than the contact pressure simulated in the above mentioned pull out tests. Thus, the staff concludes that the proposed 17-inch engagement distance (or inspection zone) is acceptable to ensure the structural integrity of the tubesheet joint.”

The NRC qualitative arguments are further supported on a more quantitative basis based on a study completed for the Model F steam generators for another plant (Reference 39)

9.1.1 Discussion of Interference Loads

There are four source terms that must be considered relative to the determination of the interface pressure between the tube and the tubesheet. These are,

1. the initial preload from the installation of the tube,
2. internal pressure in the tube that is transmitted from the ID to the OD,
3. thermal expansion of the tube relative to the tubesheet, and
4. bowing of the tubesheet that results in dilation of the tubesheet holes.

The initial preload results from the plastic deformation of the tube material relative to that of the tubesheet. The material on the inside diameter experiences more plastic deformation than the material on the outside and thus has a deformed diameter which is incrementally greater. Equilibrium of the hoop forces and moments in the tube means that the OD is maintained in a state of hoop tension at a diameter greater than a stress free state. The model for the determination of the initial contact pressure between the tube and the tubesheet, P_c , is illustrated on Figure 9-2. Both the tube and the tubesheet behave as elastic springs after the expansion process is applied. The normal stress on the tube must be equal in magnitude to the normal stress on the tubesheet and the sum of the elastic springback values experienced by each must sum to the total interference.

As long as the tube and the tubesheet remain in contact the radial normal stresses must be in equilibrium. Thus, the problem of solving for the location of the interface and the contact pressure is determinate. The elements considered in the analysis are illustrated on Figure 9-3 for all operating and postulated accident conditions; the centerline of the tube and tubesheet hole are to the left in the figure. Each source of deformation of the tube outside surface starting from the installed equilibrium condition can be visualized starting from the top left side of the figure. The sources of deformation of the tubesheet inside surface can be visualized starting from the lower left side of the figure. As illustrated, although not to scale, the tube material has a coefficient of thermal expansion that is greater than that of the tubesheet. The radial flexibility⁵, f , of the tube relative to that of the

⁵ Flexibility is the ratio of deformation to load and is the inverse of the stiffness.

tubesheet determines how much of the pressure is actually transmitted to the interface between the tube and the tubesheet. Positive radial deformation of the tube in response to an internal pressure is found as the product of the pressure, P_p , and the tube flexibility associated with an internal pressure, discussed in the next section. Thus, the tube gets tighter in the tubesheet hole as the temperature of the tube and tubesheet increase. The deformation of the tube in response to an external pressure, P_s , is the product of the pressure times the flexibility associated with an external pressure. The normal operation contact pressure, P_N , is found from compatibility and equilibrium considerations. The deformation of the tubesheet hole in response to an internal pressure, P_s , is found as the product of the pressure and the flexibility of the tubesheet associated with an internal pressure. The opening or closing of the tubesheet hole, δr_i , resulting from bow induced by the primary-to-secondary pressure difference is in addition to the deformations associated with temperature and internal pressure. Once the tube has been installed, the deformations of the tube and tubesheet associated thermal expansion, internal pressure, and tubesheet bow remain linearly elastic.

Because of the potential for a crack to be present and the potential for the joint to be leaking, the pressure in the crevice is assumed to vary linearly from the primary pressure at the crack elevation to the secondary pressure at the top of the tubesheet. If the joint is not leaking, it would be expected that there was no significant fluid pressure in the crevice. The pressure assumption is considered to be conservative because it ignores the pressure drop through the crack, and the leak path is through the crevice will not normally be around the entire circumference of the tube. In addition, the leak path is believed to be between contacting microscopic asperities between the tube and the tubesheet, thus the pressure in the crevice would not be acting over the entire surface area of the tube and tubesheet. In any event, pressure in the crevice is always assumed to be present for the analysis.

There is no bow induced increase in the diameter of the holes during normal operation or postulated accident conditions below the mid span elevation within the tubesheet, hence most analyses concentrate on locations near the top of the tubesheet. The tubesheet bow deformation under postulated accident conditions will increase because of the larger pressure difference between the bottom and top of the tubesheet. The components remain elastic and the compatibility and equilibrium equations from the theory of elasticity remain applicable. Below the mid span elevation within the tubesheet the tubesheet holes will contract. The edges of the tubesheet are not totally free to rotate and there is some suppression of the contraction near the outside radius. This also means that the dilation at the top of the tubesheet is also suppressed near the outside radius of the tubesheet. The maximum hole dilations occur near the center of the tubesheet.

The application of the theory of elasticity means that the individual elements of the analysis can be treated as interchangeable if appropriate considerations are made. The thermal expansion of the tube can be thought of as the result of some equivalent internal pressure by ignoring Poisson effects, or that tubesheet bow could be analytically treated as an increase in temperature of the tubesheet while ignoring associated changes in material properties.

Finally, the flexibility of the outside radius of the tube in response to an internal pressure, P_{ti} , is,

$$\left[\frac{2}{1 + \frac{a.c.e}{2}} \right] \text{ Closed Tube (4)}$$

where r_{ti} is the internal radius of the tube and the tube is assumed to be closed. For an open tube the term in parentheses in the numerator is simply 2. A closed tube expands less due to Poisson contraction associated with the end cap load from the internal pressure. A summary of the applicable flexibilities is provided in Table 9-1. Note that during normal operation there is an end cap load on the tube from the secondary pressure but not from that associated with the fluid in the crevice if the joint is leaking. Both flexibilities would then be involved in calculating the radial deformation of the outside of the tube. Only the open tube flexibility is used with the pressure in the crevice for postulated accident conditions.

When the inside of the tube is pressurized, P_{ti} , some of the pressure is absorbed by the deformation of the tube within the tubesheet and some of the pressure is transmitted to the OD of the tube, P_{to} , as a contact pressure with the ID of the tubesheet. The magnitude of the transmitted pressure is found by considering the relative flexibilities of the tube and the tubesheet as,

$$\left[\frac{a.c.e}{1 + a.c.e} \right] \text{ (5)}$$

Note that the tube flexibility in response to the contact pressure is for an open tube because there is no end cap load associated with the contact pressure. The denominator of the fraction is also referred to as the interaction coefficient between the tube and the tubesheet. About 85 to 90% of the pressure internal to the tube is transmitted through the tube in Westinghouse designed SGs. However, the contact pressure is not increased by that amount because the TS acts as a spring and the interface moves radially outward in response to the increase in pressure. The net increase in contact pressure is on the order of 56.4% of the increase in the internal pressure. For example, the contact pressure between the tube and the tubesheet is increased by about 1970 psi during normal operation relative to ambient conditions. Likewise, the increase in contact pressure associated with SLB conditions is about 2250 psi relative to ambient conditions.

When the temperature increases from ambient conditions to operating conditions the differential thermal expansion of the tube relative to the tubesheet increases the contact pressure between the tube and the tubesheet. The mismatch in expansion between the tube and the tubesheet, δ , is given by,

$$\delta = (\alpha_t \Delta T_t - \alpha_c \Delta T_c) r_{to} \quad \text{Thermal Mismatch (6)}$$

where: $\alpha_t, \alpha_c =$ thermal expansion coefficient for the tube and tubesheet respectively,

$\Delta T_t, \Delta T_c =$ the change in temperature from ambient conditions for the tube and tubesheet respectively.

During normal operation the temperature of the tube and tubesheet are effectively identical to within a very short distance from the top of the tubesheet and the individual changes in temperature can usually be replaced by ΔT_t , thus,

$$\delta = (\alpha_t - \alpha_c) \Delta T_t r_{to} \quad (7)$$

The change in contact pressure due to the increase in temperature relative to ambient conditions, P_T , is given by,

$$\left[\begin{array}{c} \text{a.c.e} \\ \phantom{\text{a.c.e}} \end{array} \right] \quad (8)$$

Likewise, the same equation can be used to calculate the reduction in contact pressure resulting from a postulated reduction the temperature of the tube during a postulated SLB event.

The net contact pressure, P_C , between the tube and the tubesheet during operation or accident conditions is given by,

Net Contact Pressure
$$P_C = P_0 + P_P + P_T - P_B \quad (9)$$

where P_B is the loss of contact pressure due to dilation of the tubesheet holes, P_0 is the installation preload, P_P is the pressure induced load, and P_T is the thermal induced contact load. There is one additional term that could be considered as increasing the contact pressure. When the temperature increases the tube expands more in the axial direction than the tubesheet. This is resisted by the frictional interface between the tube and the tubesheet and a compressive stress is induced in the tube. This in turn results in a Poisson expansion of the tube radius, increasing the interface pressure. The effect is not considered to be significant and is essentially ignored by the analysis.

9.1.3 Analysis

From the preceding discussions it is apparent that the contact pressure during normal operation can be found by equating the total deformation of the outside radius of the tube, r_{to} , to the total deformation of the inside radius of the tubesheet hole, r_{ci} , where the net deformation of the outside of the tube, δ_{to} , is given by,

Tube Deformation
$$\delta_{to} = \alpha_t \Delta T_t r_{to} + P_p f_{to}^c + P_s f_{to}^c + P_N f_{to}^o \quad (10)$$

and the net deformation of the tubesheet hole, δ_{ci} , is given by,

TS Deformation
$$\delta_{ci} = \alpha_c \Delta T_c r_{ci} + P_s f_{ci}^o + \delta r_i + P_N f_{ci}^o \quad (11)$$

The inclusion of the P_N terms assures compatibility and the two net deformations must be equal. It can usually be assumed that the secondary fluid pressure does not penetrate the tubesheet hole and the terms involving P_s may be ignored. All of the terms except for the final contact pressure, P_N , are known and the tubesheet bow term, δr_i , is found from the finite element model analysis of the tubesheet. The total contact pressure during operation is then found as P_N plus P_c , the installation contact pressure. For postulated SLB conditions the solution is obtained from,

$$\alpha_t \Delta T_t r_{to} + P_p f_{tot}^c + P_N f_{too}^o = \alpha_c \Delta T_c r_{cl} + \delta r_i + P_N f_{cli}^o, \quad (12)$$

or, the total contact pressure during a postulated SLB event is given by,

$$\text{SLB Contact Pres.} \quad P_T = P_c + \frac{\alpha_t \Delta T_t r_{to} - \alpha_c \Delta T_c r_{cl} + P_p f_{tot}^c - \delta r_i}{f_{cli}^o - f_{too}^o}, \quad (13)$$

where $r_{to}=r_{ci}$. A similar expression with more terms is used to obtain the contact pressure during normal operation. The denominator of the above equation is referred to as the tube-to-tubesheet influence coefficient because it related deformations associated with the interfacing components to the interface pressure. The influence coefficient for Westinghouse Model F SG tubes is calculated using the information tabulated in Table 9-1 as $3.33 \cdot 10^{-6}$ psi/inch.

By taking partial derivatives with respect to the various terms on the right the rate of change of the contact pressure as a function of changes in those parameters can be easily calculated. For example, the rate of change of the contact pressure with the internal pressure in the tube is simply,

$$\frac{\Delta P_N}{\Delta P_p} = \frac{f_{tot}^c}{f_{cli}^o - f_{too}^o}. \quad (14)$$

Thus, the rate of change of contact pressure with internal pressure in the tube is 0.564 psi/psi. Likewise, the rate of change of the contact pressure with change in the tube temperature or tubesheet temperature is given by,

$$\frac{\Delta P_N}{\Delta T_t} = \frac{\alpha_t r_{to}}{f_{cli}^o - f_{too}^o} \quad \text{and} \quad \frac{\Delta P_N}{\Delta T_c} = -\frac{\alpha_c r_{cl}}{f_{cli}^o - f_{too}^o}, \quad (15)$$

respectively. Again using the values in Table 9-1, the rate of change of contact pressure with tube temperature is 18.3 psi/°F if there is no increase in tubesheet temperature. The corresponding change with an increase in tubesheet temperature without an increase in tube temperature is -17.36 psi/°F leave a net increase in contact pressure of 0.94 psi/°F with a uniform increase in temperature of the tube and the tubesheet.

Finally, the rate of change of contact pressure with tubesheet bow is calculated as,

$$\frac{\Delta P_N}{\Delta \delta r_{cl}} = \frac{1}{f_{cl}^o - f_{too}^o} \quad (16)$$

The effect of the dilation associated with the tubesheet bow can be calculated using the information tabulated in Table 9-1. For each 0.1 mil of diameter dilation the interface pressure is reduced on the order of 380 psi. A summary of all of the contact pressure influence factors is provided in Table 9-2. A summary of tubesheet bow induced hole dilation values is provided in Table 9-3.

9.1.4 Conclusions

Although the study was completed for a Model F SG, the results listed in Table 9-3 indicate that the effect of tubesheet bow can result in a significant average decrease in the contact pressure during postulated accident conditions above the neutral plane. However, for the most severe case in one plant, in tube R18C77, the diametral change at the worst case location is less than 0.2 mils at the H* depth during postulated accident conditions. This same type of result would be expected to be the case for the Model D-5 steam generators in Byron Unit 2 and Braidwood Unit 2. Below the neutral plane, tubesheet bow is shown not to result in any tube dilation thus supporting the NRC staff conclusion that:

“Given the neutral axis to be at approximately the mid-point of the tubesheet thickness (i.e., 10.5 inches below the TTS to 17 inches below the TTS), tubesheet bore dilation effects would be expected to further tighten the joint from 10 inches below the TTS to 17 inches below the TTS which would be the lower limit of the proposed tubesheet region inspection zone. Combined with the effects of the tube joint tightening associated with the radial differential thermal expansion and primary pressure inside the tube, contact pressure over at least a 6.5 inch distance should be considerably higher than the contact pressure simulated in the above mentioned pullout tests.”

9.2 Joint Leakage Integrity Discussion

As noted in Section 4.2, “Joint Leakage Integrity”, of Reference 9, the NRC staff reviewed the qualitative arguments developed by Westinghouse regarding the conservatism of the conclusion that a minimum 17 inch engagement length ensures that leakage during a main steam line break (MSLB) will not exceed two times the observed leakage during normal operation. The NRC staff reviewed the qualitative arguments developed by Westinghouse regarding the conservatism of the “bellwether approach”, but the NRC staff’s depth of review did not permit it to credit Westinghouse’s insights from leak test data that leak flow resistance is more sensitive to changes in joint contact pressure as contact pressure increases due to the log normal nature of the relationship. The staff was still able to conclude that there should be no significant reduction in leakage resistance when going from normal operating to accident conditions.

The basis for the Westinghouse conclusion that flow resistance varies as a log normal linear function of joint contact pressure is provided in detail below. The data from the worst case tube in a comparative study analytically supports the determination that there is at least an eight inch zone in the upper 17 inches of the tubesheet where there is an increase in joint contact pressure due to a

higher primary pressure inside the tube and changes in tubesheet bore dilation along the length of the tubes. The NRC concurs (Reference 20) that the factor of 2 increase in leak rate as an upper bound by Westinghouse is reasonable given the stated premise that the flow resistance between the tube and the tubesheet remains unchanged between normal operating and accident pressure differential. The NRC staff notes in Reference 9 that the assumed linear relationship between leak rate and differential pressure is conservative relative to alternative models such as the Bernoulli or orifice models, which assumes leak rate to be proportional to the square root of the differential pressure.

The comparative study supports the NRC staff conclusion that “considering the higher pressure loading when going from normal operating to accident conditions, Westinghouse estimates that contact pressures, and, thus, leak flow resistance, always increases over at least an 8 inch distance above 17 inches below the top of the tubesheet appears reasonable to the NRC Staff.”

9.2.1 Loss Coefficient Contact Pressure Correlation

For subsequent analyses, the loss coefficient of the flow through the tube-to-tubesheet crevice must be determined as a function of the contact pressure between the tube and tubesheet. The plot of loss coefficient versus contact pressure for the Model D5 and Model F steam generators is provided in Figure 6-6 of this report. The Model F data is taken from WCAP-15932, Revision 1 (Reference 39). Figure 6-6 shows the experimentally calculated loss coefficients for the Model D5 steam generators represented by triangles and the loss coefficients for the Model F steam generators represented by squares.

Since the Model D5 and Model F steam generators have similar geometry along the crevice path, the Model F loss coefficients that were previously calculated can be used as applicable loss coefficients for the Model D5 steam generators. However, the Model D5 steam generator tubes have an outer diameter of 0.75” while the Model F steam generator tubes have an outer diameter of 0.688”. Therefore, in order to apply the Model F loss coefficients to the Model D5 steam generators, the Model F loss coefficients must be multiplied by the ratio $0.688/0.75$, which is the ratio of the Model F circumference to the Model D5 circumference. By applying the scaling factor to the Model F loss coefficients, the results obtained are considered to be the loss coefficients that would have been obtained during the Model F testing if the Model F steam generators have 0.75” tube outer diameters rather than 0.688” tube outer diameters.

Even though Model F loss coefficients could be applied to the Model D5 steam generators, it is prudent to conduct additional tests under the Model D5 tubing and tubesheet hole conditions. Such additional test data can then be used to verify the above reasoning. Therefore, the test data for the Model D5 steam generators was analyzed to provide more data points for the loss coefficients. These new results from the Model D5 tests (Tables 9-4 and 9-5) are added to the existing data set of the Model F steam generators (see Figure 9-4). The Model F data is over the higher end of the contact pressure and the Model D5 data occupies the lower end. The two data sets merge near a contact pressure of 2,400 psi. The solid black line in Figure 9-4 provides the log-linear regression line for both the Model D5 and Model F loss coefficients while the dashed line in Figure 9-4 provides the log-linear regression line for only the Model F loss coefficients. (Note that

test trials that resulted in a leakage flow rate of zero, i.e. no leakage occurred, were excluded from the plot.) As expected, the combined trend of the Model F and Model D5 data is similar to that of the Model F data alone. This substantiates the theory that the Model F and Model D5 steam generators should possess similar leakage behavior.

Note that for contact pressures less than approximately 3,000 psi, the Model F trendline provides lower loss coefficients than the trendline for the combined Model D5 and Model F data and hence, results in larger leakage flows. Therefore, since the previously used trendline for the Model F data provided larger leakage flows than the newly revised trendline for the combined Model D5 and Model F data, the previously used Model F trendline is more conservative than the newly developed trendline for the combined Model D5 and Model F data at pressures less than 3,000 psi. (Note that a pressure of greater than 3,000 psi is only inflicted upon the steam generator during a 3,110 psi hydro-test and is never reached during normal or steam line break operations.) Therefore, the previously completed Model F H* analyses were performed conservatively compared to the newly developed approach and hence, the previously completed Model F H* analyses are valid and are not required to be recalculated.

A linear regression and an uncertainty analysis were performed for the combined Model D5 and Model F steam generator data. Figure 6-6 provides a plot of the loss coefficient versus contact pressure with the linear regression trendline for the combined data represented as a thick, solid black line. The regression trendline is approximated by the following log-linear relation.

$$\text{Log}_{10}(K) = A\sigma_c + B \quad (17)$$

where

A = slope of log-linear regression trendline

B = y-intercept of log-linear regression trendline

The parabolic curve that provides the 95% confidence lower bound for the data in Figure 9-4 is represented as a dashed curve. The 95% confidence lower bound curve is approximated by the following log-parabolic relation.

$$\text{Log}_{10}(K) = A\sigma_c^2 + B\sigma_c + C \quad (18)$$

where

A = coefficient of second order term

B = coefficient of first order term

C = y-intercept of log-parabolic curve

The table below summarizes the log-linear regression trendline parameters and the 95% confidence log-parabolic curve parameters for the combined Model D5 and Model F steam generator data.

	Coefficient of Second Order Term	Coefficient of First Order Term	Y-Intercept of Curve
Log-Linear Regression Trendline	0	2.167×10^{-4}	12.232
95% Confidence Lower Bound Curve	-7.891×10^{-8}	5.265×10^{-4}	11.756

Therefore, the log-linear fit to the combined Model D5 and Model F loss coefficient data follows the equation

$$\text{Log}_{10}(K) = (2.167 \times 10^{-4})\sigma_c + 12.232 \quad (19)$$

while the 95% lower bound confidence limit for the combined Model D5 and Model F data follows the equation

$$\text{Log}_{10}(K) = (-7.891 \times 10^{-8})\sigma_c^2 + (5.265 \times 10^{-4})\sigma_c + 11.756 \quad (20)$$

Table 9-1.
Radial Flexibilities Times Elastic Modulus (in./psi)

a.c.c

Table 9-2.
Contact Pressure Influence Factors for Model F SG Tubes at 600°F

a,c,e

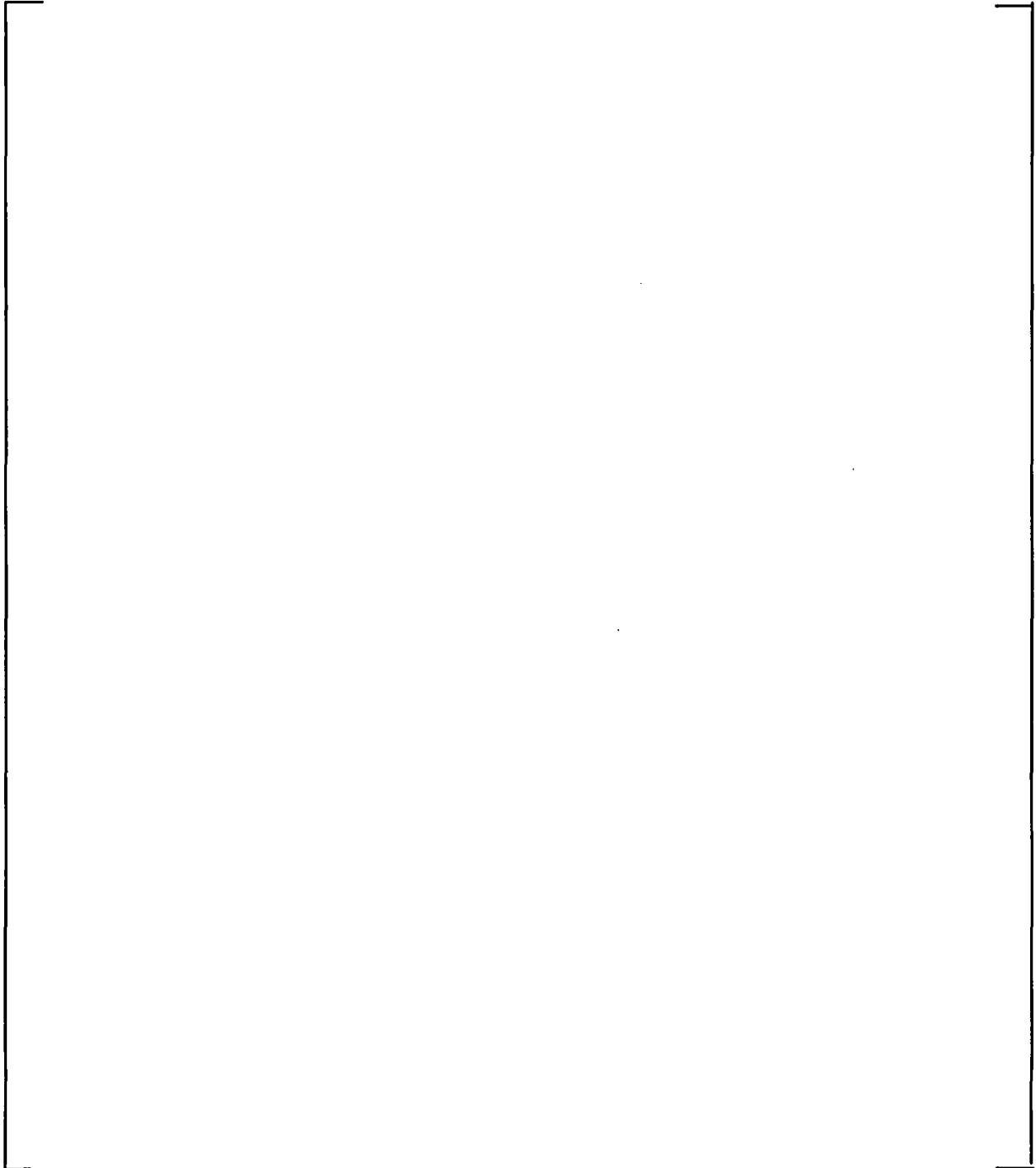
Table 9-4.
Contact Pressure for Experimental Loss Coefficients at Room Temperature Conditions

a.c.e

--

Table 9-5.
Contact Pressure for Experimental Loss Coefficients at 600°F Heated Conditions

a.c.c



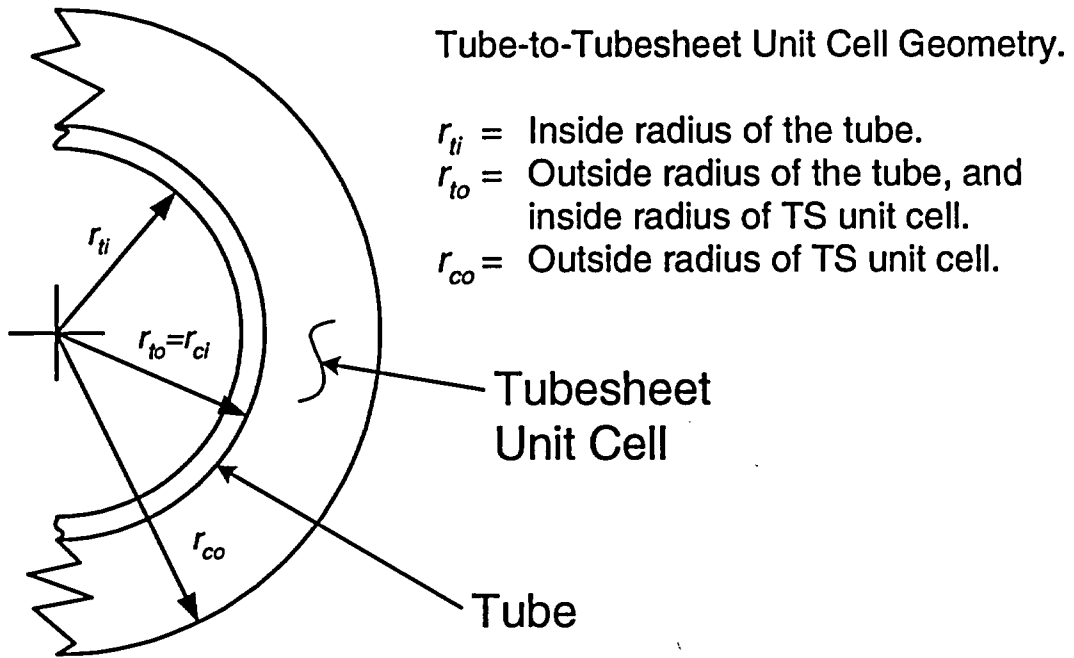


Figure 9-1. Geometry of the Tube-to-Tubesheet Interface

a.c.c



Figure 9-2. Model for Initial Contact Pressure



Figure 9-3. Determination of Contact Pressure, Normal or Accident Operation

(As illustrated, the bow does not result in a loss of contact, however, there are situations where the bow is sufficient to result in a loss of contact between the tube and the tubesheet at the top of the tubesheet.)



Figure 9-4.
Loss Coefficient versus Contact Pressure for Model D5 and Model F Steam Generators

10.0 Conclusions and Inspection Recommendations

The evaluation in Section 8.0 of this report provides a technical basis for bounding the potential leak rate from non-detected indications in the tube region below 17 inches from the top of the tubesheet as no more than twice the leak rate during normal operation. This applies equally to any postulated indications in the tack expansion region and in the tube-to-tubesheet welds. If cracks are found within the specified inspection depth, it is recommended that the inspection be expanded to include 100% of the tubes in the affected SG using that same specified inspection depth, e.g., 17 inches, as discussed in item 4 of Section 12.0. If the cracking is identified at an existing bulge or over expansion location, the scope expansion can be limited to the population of identified bulges and over expansions within the inspection region. As noted in the introduction to this report, the reporting of crack-like indications in the tube-to-tubesheet welds would be expected to occur inadvertently since no structural or leak rate technical reason exists for a specific examination to take place.

The evaluations performed as reported herein have demonstrated that:

- 1) There is no structural integrity concern associated with tube or tube weld cracking of any extent provided it occurs below the H^* distance as reported in Section 7.0 of this report. The pullout resistance of the tubes has been demonstrated for axial forces associated with 3 times the normal operating differential pressure and 1.4 times differential pressure associated with the most severe postulated accident.
- 2) Contact forces during postulated LOCA events are sufficient to resist axial motion of the tube. Also, if the tube end welds are not circumferentially cracked, the resistance of the tube-to-tubesheet hydraulic joint is not necessary to resist push-out. Moreover, the geometry of any postulated circumferential cracking of the weld would result in a configuration that would resist pushout in the event of a loss of coolant accident. In other words, the crack flanks would not form the cylindrical surface necessary such that there would be no resistance to expulsion of the tube in the downward direction.
- 3) The leak rate for indications below the neutral plane of the tubesheet is expected to be bounded on average by twice the leak rate that is present during normal operation of the plant.
- 4) The leak rate for indications below a depth of about 17 inches from the top of the tubesheet would be bounded by twice the leak rate that is present during normal operation of the plant regardless of tube location in the bundle. This is apparent from comparison of the contact pressures from the finite element analyses over the full range of radii from the center of the tubesheet, and ignores any increase in the leak rate resistance due to the contact pressure changes and associated tightening of the crack flanks.

The recommendations with regard to the inspection of the welds at Braidwood 2 and Byron 2 are based on the following:

-
- 1) Examination of the tubes below the H* elevations as described in Reference 5 could be omitted based on structural considerations alone if a license amendment were obtained to that effect.
 - 2) Similar considerations lead to the conclusion that the leak rate during postulated faulted events would be bounded by twice the leak rate during normal operation and the examination of the tube below the specified inspection depth of 17 inches (which includes the tack expansions and the welds) can be omitted from consideration.
 - 3) The prior conclusions rely on the inherent strength and leak rate resistance of the hydraulically expanded tube-to-tubesheet joint, a feature which was not considered or permitted to be considered for the original design of the SG. Thus, omission of the inspection of the weld constitutes a reassignment of the pressure boundary to the tube-to-tubesheet interface. Similar considerations for tube indications require NRC staff approval of a license amendment.

Based on the summary discussion, Westinghouse has reviewed and endorses the following SG tubes inspection plan on a permanent basis with regard to the tubesheet region in each SG for the Braidwood 2 and Byron 2 steam generators:

1. Perform a 20% inspection of the hot leg side tubes using RPC technology from 3 inches above the top of the tubesheet to 3 inches below the top of the tubesheet. Expand to 100% of the affected SG in this region only if cracking is found that is not associated with a bulge or overexpansion as described below.
2. Perform a 20% inspection of the hot leg side tubes using RPC technology for depths indicated down to the top of the tubesheet minus 17 inches for indications of bulges ≥ 18 Volts and over expansions ≥ 1.5 mils on the diameter, as obtained from a review of the cycle 10 data for Braidwood 2 and cycle 11 data for Byron 2. Note, the 20% sample could be developed by examining 20% of the parent tube population and biasing the selection process to assure that at least 20% of the bulge and over expansion indications within the 17 inch length were also sampled. It is also noted that the inspection of a single tube can simultaneously contribute to meeting the scope of both inspection items 1 and 2.
3. If cracking is found in the sample population of bulges or over expansions, the inspection scope should be increased to 100% of the population of bulge and overexpansion locations for the region of the top of the tubesheet to a depth of 17 inches in the affected SG.
4. If cracking is reported at one or more tube locations not designated as either a top of the tubesheet expansion transition, a bulge or an over expansion, an engineering evaluation can be performed aimed at determining the cause for the signal, e.g., some other tubesheet anomaly, in order to identify a critical area for the expansion of the inspection. This inspection will be limited to the original specified depth of 17 inches.

11.0 References

1. OE19662 (Restricted & Confidential), "Steam Generators (Catawba Nuclear Power Station)," Institute of Nuclear Power Operations (INPO), Atlanta, GA, USA, December 13, 2004.
2. IN 2005-09, "Indications in Thermally Treated Alloy 600 Steam Generator Tubes and Tube-to-Tubesheet Welds," United States Nuclear Regulatory Commission, Washington, DC, publication date to be determined, April 7, 2005.
3. SGMP-IL-05-01, "Catawba Unit 2 Tubesheet Degradation Issues," EPRI, Palo Alto, CA, March 4, 2005.
4. OE20339, "Vogtle Unit 1 Steam Generator Tube Crack Indications," Institute of Nuclear Power Operations (INPO), Atlanta, GA, USA, April 4, 2005.
5. WCAP-16152, "Justification of the Partial-Length Rotating Pancake Coil (RPC) Inspection of the Tube Joints of the Byron/Braidwood Unit 2 Model D5 Steam Generators," Westinghouse Electric Company LLC, Pittsburgh, PA, December 2003.
6. 1003138, "EPRI PWR SG Examination Guidelines: Revision 6," EPRI, Palo Alto, CA, October 2002.
7. ASME Boiler and Pressure Vessel Code, Section III, "Nuclear Power Plant Components," American Society of Mechanical Engineers, New York, New York, 1971, Summer 1972 Addenda and selected sections of the Winter 1974 addenda.
8. GL 2004-01, "Requirements for Steam Generator Tube Inspections," United States Nuclear Regulatory Commission, Washington, DC, August 30, 2004.
9. NRC Letter, "Braidwood Station, Units 1 and 2 – Issuance of Exigent Amendments Re: Revision of Scope of Steam Generator Inspections for Unit 2 Refueling Outage 11 – (TAC Nos. MC6686 and MC6687)," United States Nuclear Regulatory Commission, Washington, DC, April 25, 2005.
10. NEI 97-06, Rev. 1, "Steam Generator Program Guidelines," Nuclear Energy Institute, Washington, DC, October 2000.
11. RG 1.121 (Draft), "Bases for Plugging Degraded PWR Steam Generator Tubes," United States Nuclear Regulatory Commission, Washington, DC, August 1976.
12. Federal Register, Part III, Nuclear Regulatory Commission, National Archives and Records Administration, Washington, DC, pp. 10298 to 10312, March 2, 2005.
13. WNET-153 (Proprietary), "Model D5 Steam Generator Stress Report Commonwealth Edison Company Byron Station 2," Westinghouse Electric Company LLC, Pittsburgh, PA, June 1982.
14. WNEP-8425 (Proprietary), "Model D5 Steam Generator Stress Report for Commonwealth Edison Company Braidwood Unit 2," Westinghouse Electric Company LLC, Pittsburgh, PA, March 1984.

-
15. ASME Boiler and Pressure Vessel Code, Section XI, "Rules for Inservice Inspection of Nuclear Power Plant Components," American Society of Mechanical Engineers, New York, New York, 1971.
 16. ASME Boiler and Pressure Vessel Code, Section XI, "Rules for Inservice Inspection of Nuclear Power Plant Components," American Society of Mechanical Engineers, New York, New York, 2004.
 17. WCAP-11224, Rev. 1, "Tubesheet Region Plugging Criterion for the Duke Power Company McGuire Nuclear Station Units 1 and 2 Steam Generators," Westinghouse Electric Company LLC, Pittsburgh, PA, October 1986.
 18. WCAP-13532, Rev. 1, "Sequoyah Units 1 and 2 W* Tube Plugging Criteria for SG Tubesheet Region of WEXTX Expansions," Westinghouse Electric Company LLC, Pittsburgh, PA, 1992.
 19. WCAP-14797, "Generic W* Tube Plugging Criteria for 51 Series Steam Generator Tubesheet Region WEXTX Expansions," Westinghouse Electric Company LLC, Pittsburgh, PA, 1997.
 20. "Safety Evaluation by the Office of Nuclear Reactor Regulation Related to Amendment No. 129 to Facility Operating License No. DPR-80 and Amendment No. 127 to Facility Operating License No. DPR-82 Pacific Gas and Electric Company Diablo Canyon Nuclear Power Plant, Units 1 and 2 Docket Nos. 50-275 and 50-323," United States Nuclear Regulatory Commission, Washington, DC, 1999.
 21. NSD-RFK-96-015, "Vogtle 1 Tube Integrity Evaluation, Loose Part Affected SG," Westinghouse Electric Company LLC, Pittsburgh, PA, June 9, 1996.
 22. Calculation Note CN-SGDA-03-85, Rev. 1 "H*/P* Input for Model D5 and Model F Steam Generators," September 2003 (Proprietary Report).
 23. Calculation Note CN-SGDA-08-87, October 2003 (Proprietary Report.)
 24. WCAP-16932-P (Proprietary), Rev. 1, Improved Justification of Partial-Length RPC Inspection of the Tube Joints of Model F Steam Generators of Ameren-UR Callaway Plant," Westinghouse Electric Company LLC, Pittsburgh, PA, May 2003.
 25. NSD-E-SGDA-98-3611 (Proprietary), "Transmittal of Younggwang Unit 2 Nuclear Power Plant Steam Generator Tube-to-Tubesheet Joint Evaluation," Westinghouse Electric Company LLC, Pittsburgh, PA, November 1998.
 26. Porowski, J.S. and O'Donnell, W.J., "Elastic Design Methods for Perforated Plates," Transactions of the ASME Journal of Engineering for Power, Vol. 100, p. 356, 1978.
 27. Slot, T., "Stress Analysis of Thick Perforated Plates," Ph.D Thesis, Technomic Publishing Co., Westport, CN 1972.
 28. Computer Program WECAN/Plus, "User's Manual," 2nd Edition, Revision D, Westinghouse Government Services LLC, Cheswick, PA, May 1, 2000.
 29. SM-98-102 (Proprietary), Rev. 2, "Tube/Tubesheet Contact Pressures for Yonggwang 2," Westinghouse Electric Company LLC, Pittsburgh, PA, November 1998.

-
30. Nelson, L.A., "Reference for Model D Tubesheet Simulate of 1.800 Inch Diameter, electronic mail (Contained in Reference 31), Westinghouse Electric Company LLC, Pittsburgh, PA, August 6,2003.
 31. CN-SGDA-03-87 (Proprietary), "Evaluation of the Tube/Tubesheet Contact Pressures and H* for Model D5 Steam Generators at Byron, Braidwood, Catawba and Comanche Peak," Westinghouse Electric Company LLC, Pittsburgh, PA, October 2003.
 32. ASME Boiler and Pressure Vessel Code Section III, "Rules for Construction of Nuclear Power Plant Components," 1989 Edition, The American Society of Mechanical Engineers, New York, NY.
 33. CN-SGDA-03-85 (Proprietary), Rev. 1, "H*/P* Input for Model D5 and Model F Steam Generators," Westinghouse Electric Company LLC, Pittsburgh, PA, September 2003.
 34. CN-SGDA-02-152 (Proprietary), Rev. 1, "Evaluation of the Tube-to-Tubesheet Contact Pressures for Callaway Model F Steam Generators," Westinghouse Electric Company LLC, Pittsburgh, PA, March 2003.
 35. CN-SGDA-03-37 (Proprietary), "Evaluation of the Tube/Tubesheet Contact Pressures and H* for Model D-5 Steam Generators at Byron, Braidwood, Catawba and Comanche Peak," Westinghouse Electric Company LLC, Pittsburgh, PA, October 2003.
 36. CN-SGDA-03-133 (Proprietary), Rev. 0, "Evaluation of the H* Zone Boundaries for Specific Model D-5 and Model F Steam Generators," Westinghouse Electric Company LLC, Pittsburgh, PA, October 2003.
 37. WNET-153, Vol. 5 (Proprietary), "Model D-5 Steam Generator Stress Report: Tube Analysis," Westinghouse Electric Company LLC, Pittsburgh, PA, March 1982.
 38. CN-SGDA-03-121, "H* Ligament Tearing for Models F and D5 Steam Generators," 10/03 (Proprietary Report).
 39. WCAP 15932-P, Revision 1, "Improved Justification of Partial-Length RPC Inspection of Tube Joints of Model F Steam Generators of Ameren-UE Callaway Plant," Westinghouse Electric Company LLC, Pittsburgh, PA May 2003